Cellular Microbiology (2007) 9(9), 2112–2125

doi:10.1111/j.1462-5822.2007.00941.x
First published online 17 April 2007

# Rab11B small GTPase regulates secretion of cysteine proteases in the enteric protozoan parasite *Entamoeba histolytica*

**Biswa Nath Mitra,[1] Yumiko Saito-Nakano,[2] Kumiko Nakada-Tsukui,[1] Dan Sato[1] and Tomoyoshi Nozaki[1]***

[1]*Department of Parasitology, Gunma University Graduate School of Medicine, 3-39-22 Showa-machi, Maebashi, Gunma 371-851, Japan.*

[2]*Department of Parasitology, National Institute of Infectious Diseases, 1-23-1 Toyama, Shinjuku-ku, Tokyo 162-8640, Japan.*

## Summary

**Vesicular trafficking plays a pivotal role in the virulence of the enteric protozoan parasite *Entamoeba histolytica*. In the present study, we showed that one isotype of the small GTPase Rab11, *Eh*Rab11B, plays a central role in the secretion of a major virulence factor, cysteine proteases. *Eh*Rab11B did not colocalize with markers for the endoplasmic reticulum, early endosomes and lysosomes, but was partially associated with non-acidified vesicles in the endocytic pathway, likely recycling endosomes. Overexpression of *Eh*Rab11B resulted in a remarkable increase in both intracellular and secreted cysteine protease activity, concomitant with an augmentation of cytolytic activity as demonstrated by an increased ability to destroy mammalian cells. The oversecretion of cysteine proteases with *Eh*Rab11B overexpression was neither sensitive to brefeldin A nor specific to a certain cysteine protease species (e.g. CP1, 2 or 5), suggesting that these three major cysteine proteases are trafficked via an *Eh*Rab11B-associated secretory pathway, which is distinct from the classical brefeldin-sensitive pathway. Overexpression of *Eh*Rab11B also enhanced exocytosis of the incorporated fluid-phase marker, supporting the notion that it is involved in recycling. This is the first report demonstrating that Rab11 plays a central role in the transport and secretion of pathogenic factors.**

Received 1 November, 2006; revised 7 February, 2007; accepted 23 February, 2007. *For correspondence. E-mail nozaki@med.gunma-u.ac.jp; Tel. (+81) 27 220 8020; Fax (+81) 27 220 8025.



## Introduction

Rab proteins are members of the Ras super-family of small GTPases and essential to the regulation of vesicular trafficking in the endocytic and exocytic/secretory pathways in eukaryotic cells (Zerial and McBride, 2001). Rab GTPases are localized to discrete membrane-bound compartments, where they have a specific role depending on the kind and location of Rab (Novick and Zerial, 1997; Chavrier and Goud, 1999). From fission yeast to mammals and higher plants, the Rab family has expanded significantly; the diversity of these proteins is often regarded as a reflection of membrane trafficking complexity (Zerial and McBride, 2001). The human genome contains more than 60 Rabs, while the genomes of the fruit fly, nematode and yeast have 26, 29 and 11 Rabs, respectively (Bock *et al.*, 2001). Some Rabs, e.g. Rab5 and Rab7, are ubiquitous (Stenmark and Olkkonen, 2001), while others, e.g. Rab3 (Schluter *et al.*, 2002) and Rab27A (Hume *et al.*, 2001; Stinchcombe *et al.*, 2001), are unique to particular cells, tissues, organs and species (Seabra *et al.*, 2002). Rab11 is one of the ubiquitous Rabs, distributed in the trans-Golgi network (TGN), post-Golgi vesicles and recycling endosomes (Urbe *et al.*, 1993; Ullrich *et al.*, 1996; Ren *et al.*, 1998; McNiven and Thompson, 2006). In Chinese hamster ovary (CHO) cells, Rab11 was shown to regulate the recycling of the transferrin receptor to the plasma membrane (Ullrich *et al.*, 1996; Ren *et al.*, 1998). In parietal epithelial cells, Rab11 was also shown to control the cell surface expression of $H^+/K^+$ ATPase by regulating recycling to the plasma membrane (Goldenring *et al.*, 1994). Rab11 was also implicated in the transport from the Golgi apparatus to plasma membrane (Chen *et al.*, 1999). In yeast, two Rab11 homologues, Ypt31p and Ypt32p, were assumed to regulate the secretory pathway as a *ypt31/ypt32*-mutant was unable to secrete invertase (Benli *et al.*, 1996). In addition to recycling and exocytosis, Rab11 regulates transport from early endosomes to TGN (Wilcke *et al.*, 2000), suggesting that it may interconnect the endocytic and secretory pathways (Somsel Rodman and Wandinger-Ness, 2000; Savina *et al.*, 2002; Fader *et al.*, 2005). In the protozoan parasite *Trypanosoma brucei*, Rab11 was shown to be developmentally regulated and involved in the recycling of

transferrin receptors (ESAG6 and 7) (Jeffries *et al.*, 2001). In a non-pathogenic soil-amoeba, *Dictyostelium discoideum*, Rab11 was found to be associated with and regulate the structure and functions of the contractile vacuole system (Harris *et al.*, 2001).

The enteric protozoan parasite *Entamoeba histolytica* is a causative agent of an estimated 50 million cases of amoebic dysentery, colitis and liver abscess in humans, which leads to 100 000 deaths annually (Stanley *et al.*, 1995). This unicellular protist has 91–105 Rab genes (Lal *et al.*, 2005; Saito-Nakano *et al.*, 2005) despite its small genome (20 Mb) (Loftus *et al.*, 2005) and a simple life cycle, consisting of only two developmental stages, the disease-causing trophozoites and the dormant cysts (Eichinger, 1997). Vesicular trafficking plays a critical role in the parasitic life style and virulence of *E. histolytica*. Developmental changes, i.e. encystation and excystation, which require drastic morphological and biochemical changes, are accompanied by a radical reorganization of organelles and the synthesis, sorting and degradation of a large number of proteins. In the intestinal lumen and the tissues, the trophozoites actively absorb nutrients by degrading endocytosed macromolecules and also by engulfing and degenerating phagocytosed microorganisms and host cells. In addition, to establish a microenvironment suitable for colonization, they secrete various hydrolytic and membranolytic factors including cysteine proteases (Que and Reed, 2000) and the pore-forming peptide amoebapore (Leippe, 1999). Cysteine proteases compose a family of 44 members (Tillack *et al.*, 2006), and are currently considered primarily responsible for the pathogenesis. CP1 and CP5 were shown to be absent or degenerated in a closely related but non-pathogenic *Entamoeba dispar* species (Bruchhaus *et al.*, 1996; Willhoeft *et al.*, 1999). Overexpression of CP2 caused an augmentation of the destruction of cell monolayers, but no change in the formation of abscesses in the liver (Hellberg *et al.*, 2001). Antisense inhibition of CP5 resulted in a reduced capacity of liver abscess formation (Ankri *et al.*, 1999) and a reduced production of the inflammatory cytokines interleukin 1β and interleukin 8 by intestinal epithelial cells (Zhang *et al.*, 2000). It was also shown that in patients with invasive amoebiasis, there is a correlation among the levels of extracellular cysteine protease, epithelial damage and production of anticysteine protease antibodies (Reed *et al.*, 1989).

Although an understanding of the biosynthesis and transport of cysteine proteases is essential for comprehending the virulence of this parasite and also for the development of measures to intervene in its transmission, the molecular mechanisms of cysteine protease transport have only started to be unveiled (Temesvari *et al.*, 1999; McGugan and Temesvari, 2003; Saito-Nakano *et al.*, 2004; 2007; Nakada-Tsukui *et al.*, 2005; Saric *et al.*, 2006; Sato *et al.*, 2006). It was previously shown that cysteine proteases were abundant in the early and late endosomes, and colocalized with *Eh*Rab7A and *Eh*Rab11A, suggesting these Rabs to be involved in their transport (Temesvari *et al.*, 1999). We previously showed that the transport of cysteine proteases during phagocytosis is regulated by *Eh*Rab5 and *Eh*Rab7A (Saito-Nakano *et al.*, 2004; Nakada-Tsukui *et al.*, 2005). These two Rabs are involved in the formation of an unique preparatory compartment, the 'prephagosomal vacuole', which likely serves as a site for the processing, activation and temporary storage of cysteine proteases targeted at phagosomes. We also showed that the targeting of cysteine proteases is mediated by *Eh*Rab7A, and the interaction of *Eh*Rab7A with the retromer-like complex indirectly controls the efficiency with which cysteine proteases are transported to lysosomes. Furthermore, we have recently shown that the transport of cysteine proteases to lysosome was regulated by another member of Rab7 isotypes, *Eh*Rab7B (Saito-Nakano *et al.*, 2007). However, the expression of neither wild type nor mutant forms of *Eh*Rab5, *Eh*Rab7A and *Eh*Rab7B resulted in drastic changes in transport, suggesting the presence of other Rab(s) that play a crucial role in the process.

*E. histolytica* possesses four Rab11 homologues, *Eh*Rab11A (Temesvari *et al.*, 1999; McGugan and Temesvari, 2003), *Eh*Rab11B, *Eh*Rab11C (Saito-Nakano *et al.*, 2001; 2005) and *Eh*Rab11D (Saito-Nakano *et al.*, 2005), which show 55–63% mutual identity (Saito-Nakano *et al.*, 2005). It has been suggested that *Eh*Rab11A plays a role in the transport during starvation and encystation as it is concentrated at the periphery of the cell under these conditions (McGugan and Temesvari, 2003). In this study, we characterized the second member of the Rab11 gene family, *Eh*Rab11B. We showed that *Eh*Rab11B plays a pivotal role in the transport and secretion of the major cysteine proteases, and cytolytic activity against mammalian cells.

## Results

### *Expression of EhRab11 isotypes measured by quantitative real-time (RT) polymerase chain reaction (PCR)*

In order to see relative levels of the mRNA of Rab11 isotypes in *E. histolytica*, the amounts of a steady state transcript of *Eh*Rab11A-D, as well as *Eh*Rab5 and *Eh*Rab7A, in the trophozoite stage were measured by quantitative RT-PCR with RNA polymerase II 15 kDa subunit as an internal control (Fig. 1). The relative mRNA level of *Eh*Rab11B was approximately 67–74% that of *Eh*Rab11A and *Eh*Rab7A, and significantly higher than levels of the other two *Eh*Rab11 isotypes (*Eh*Rab11C and *Eh*Rab11D) and *Eh*Rab5.

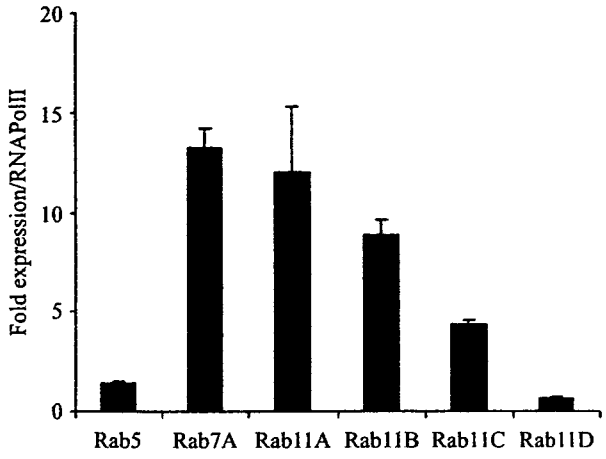


**Fig. 1.** Relative expression of *Eh*Rab11 in *E. histolytica*. Trophozoites in the logarithmic growth phase were harvested for the extraction of total RNA and synthesis of cDNA. The RT-PCR was performed as described in *Experimental procedures*, and the expression levels are shown relative to the amount of RNA polymerase. Error bars represent the standard error of the mean of three independent experiments.

### *Subcellular distribution of EhRab11B*

Rab GTPases perform their respective functions in confined intracellular compartments. To understand the different functions of Rab11 isotypes in *E. histolytica*, we first examined the intracellular distribution of *Eh*Rab11B using the amoebic transformant that expressed HA-tagged *Eh*Rab11B. HA-tagged *Eh*Rab11B appeared to be associated with membranes or dot-like structures scattered throughout the cytosol. When the transformant was incubated with the fluid-phase marker FITC-dextran for 10 or 30 min and subjected to an immunofluorescence assay using anti-HA antibody, no vesicle/vacuole was simultaneously labelled with both FITC-dextran and anti-HA antibody (data not shown). Next, the HA-*Eh*Rab11B transformant was incubated with FITC-dextran for 60 min and then chased in a marker-free medium for 120 min. We observed a partial colocalization of FITC-dextran and *Eh*Rab11B (Fig. 2). We quantified the colocalization with two parameters: the percentage of trophozoites that contained FITC-dextran- and *Eh*Rab11B double-positive vesicles/vacuoles and the percentage of FITC-dextran- and *Eh*Rab11B double-positive vesicles/vacuoles among FITC-dextran-labelled vesicles/vacuoles. These two parameters showed similar kinetics; they gradually increased up to 60 min of chase, and then decreased at 120 min (Fig. 2B and C). We verified the localization and kinetics of *Eh*Rab11B during endocytosis using the wild-type strain and antibody raised against the recombinant *Eh*Rab11B to obtain comparable results (data not shown). We stained the *Eh*Rab11B transformant with LysoTracker Red, and rarely found the colocalization of *Eh*Rab11B and the acidic compartment labelled with LysoTracker (data not shown). We also carried out an immunofluorescence assay using a transformant that expressed CP5 with a HA-tag at the carboxyl terminus (Sato *et al.*, 2006) and anti-HA and anti-*Eh*Rab11B antibodies (Fig. 3A). We observed a partial colocalization of epitope-tagged CP5 and endogenous *Eh*Rab11B. The HA-*Eh*Rab11B-expressing transformant was also stained with antibody against the Sec61 α-subunit and dolicol-*P*-mannose synthase (DPMS), markers for the endoplasmic reticulum, showing no apparent colocalization with *Eh*Rab11B (Fig. 3B and C).

We further investigated if *Eh*Rab11B is involved in the transport to and/or maturation of lysosomes. We examined the acidity of whole amoebae by measuring the fluorescence intensity of the LysoTracker-stained acidic compartment of the *Eh*Rab11B-overexpressing and control transformants in a FACS-based analysis. We found no difference in the volume of the acidic compartment between these two transformants (data not shown). The results suggest that *Eh*Rab11B is not primarily associated with either late endosomes or lysosomes but confined to a compartment that only partially overlaps the endocytic and/or recycling pathway.

### *Overexpression of EhRab11B was accompanied by a dramatic increase of cysteine protease activity*

It has been well established that secreted cysteine proteases play an indispensable role in amoebic invasion and tissue destruction due to their hydrolytic and degradative activities towards extracellular matrix proteins (Stanley *et al.*, 1995). We investigated the effects of the overexpression of *Eh*Rab11B on the secretion of cysteine proteases. We first examined the degree of overexpression (i.e. fold increase) in the HA-*Eh*Rab11B transformant compared with the control transformant (Fig. 4A). We estimated that the *Eh*Rab11B protein level increased by approximately ninefold as estimated from quantification of fluorescent signals by chemiluminescence detection with immunoblots obtained using anti-*Eh*Rab11B antibody (data not shown).

We examined cysteine protease activity in the lysate and culture supernatant of the HA-*Eh*Rab11B-overexpressing transformant, by measuring hydrolysis of the synthetic peptide substrate, z-Arg-Arg-7-amino-4-trifluoromethylcoumarin (Fig. 4B and C). It has been well established that the amoebic cysteine proteases have a strong preference for peptides containing Arg residues at the P1 and P2 positions (Jacobs *et al.*, 1998). Cysteine protease activity was 15-fold higher in the culture supernatant of the *Eh*Rab11B-overexpressing transformant than that of the control transformant ($P < 0.001$; Fig. 4C). Similarly, the total cysteine protease activity in the lysate of the *Eh*Rab11B-overexpressing transformant was 2.6-fold the control level ($P < 0.005$; Fig. 4B). The observed protease

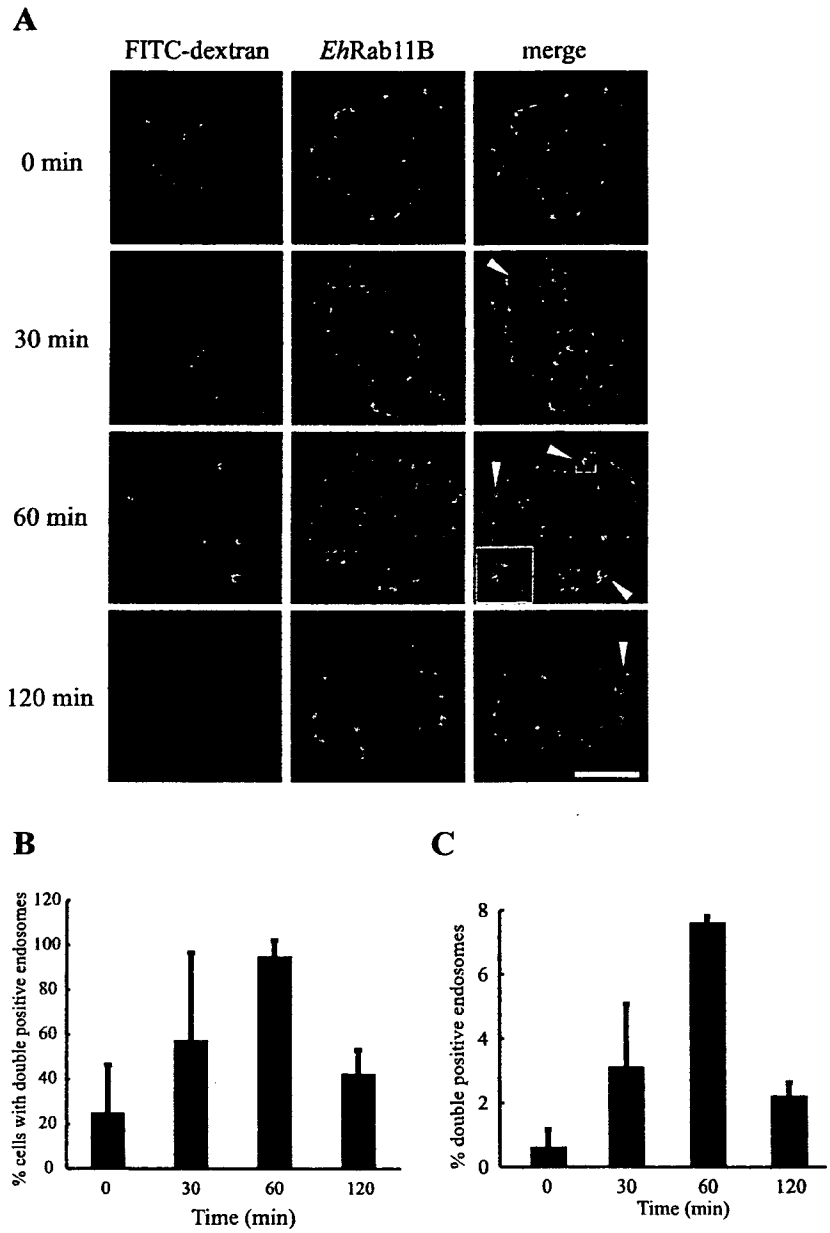


**Fig. 2.** Colocalization of *Eh*Rab11B and the fluid-phase marker.
A. The amoebae were pulsed with FITC-dextran for 1 h and further chased for the periods indicated (0, 30, 60 and 120 min). Images of immunofluorescence using anti-HA antibody to probe 3HA-tagged *Eh*Rab11B (red) together with FITC-dextran (green) are shown. White arrowheads indicate endocytosed FITC-dextran colocalized with *Eh*Rab11B. The islet shows a magnified image. Bar, 10 μm.
B. The percentage of trophozoites containing at least one FITC-dextran/*Eh*Rab11B double-positive vesicle/vacuole is shown.
C. The proportion of FITC-dextran/*Eh*Rab11B double-positive vesicles/vacuoles among all FITC-dextran-positive endosomes is shown. Error bars represent the standard error of the mean of two independent experiments.

activity was completely abolished when trophozoites were pretreated with 200 μM of E64, a potent, irreversible and highly selective cysteine protease inhibitor (Jacobs *et al.*, 1998; Que *et al.*, 2002) (data not shown).

To confirm these results and further determine which cysteine protease isotypes were over-produced and secreted, we performed gelatin substrate gel electrophoresis. The lysates (Fig. 4D) and culture-supernatant (Fig. 4E) of the *Eh*Rab11B-overexpressing and control transformants yielded zymograms of three predominant bands of cysteine protease activity in the range of 29–60 kDa on SDS-PAGE under non-reducing conditions, likely corresponding to CP1, 2 and 5, consistent with previous findings (Hellberg *et al.*, 2000). Although the ratio of the three major cysteine protease bands could not be determined, all three bands in both the lysate and supernatant appeared more intense in the *Eh*Rab11B-overexpressing transformant than control transformant, with the intensity of the band corresponding to CP1 increasing most remarkably among the three cysteine proteases. All three bands were abolished when trophozoites were pretreated with 200 μM E64 (data not shown).

It has been recently shown that cysteine proteases are transported via the brefeldin A (BFA)-insensitive route inducible by external stimuli (Manning-Cela *et al.*, 2003). To see if the augmented secretion of cysteine proteases in

 

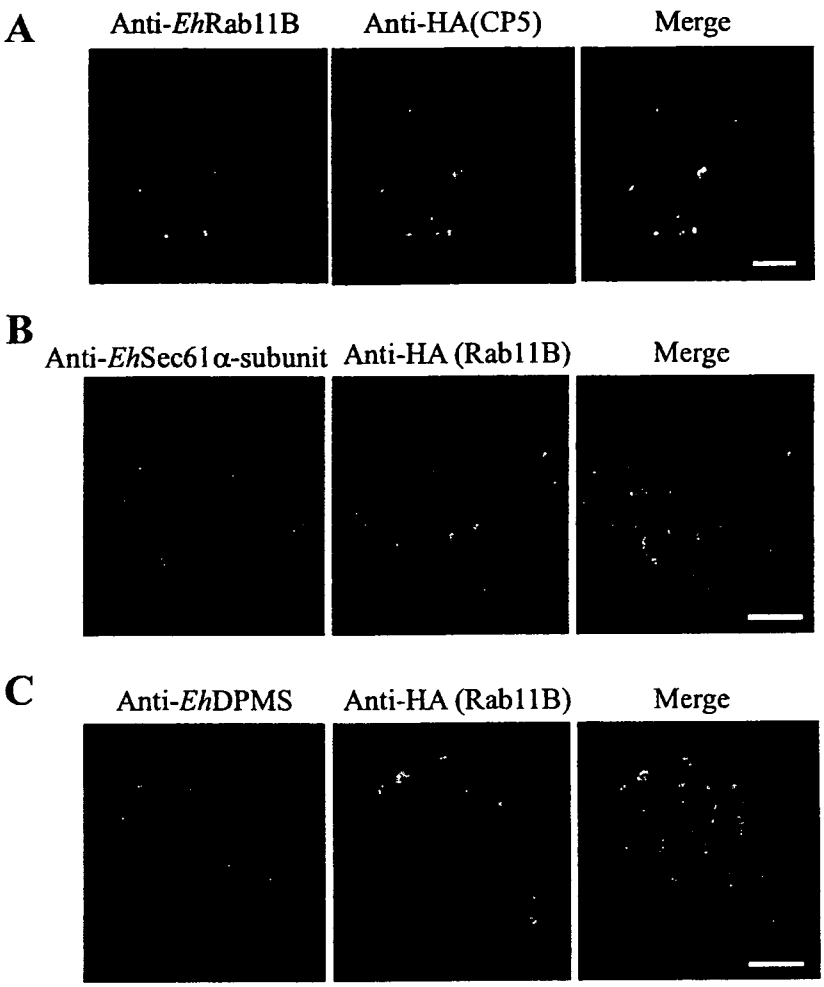


**Fig. 3.** *Eh*Rab11B is partially associated with CP5, and not associated with the endoplasmic reticulum.
A. Partial colocalization of *Eh*Rab11B and CP5. An immunofluorescence assay was conducted using a transformant that expressed CP5 with a HA-tag at the carboxyl terminus (Sato *et al.*, 2006) and anti-HA and anti-*Eh*Rab11B antibodies.
B and C. Lack of colocalization of *Eh*Rab11B and the markers for the endoplasmic reticulum. The *Eh*Rab11B-overexpressing transformant was stained with anti-*Eh*Sec61 α-subunit (B, green)or anti-*Eh*DPMS (C, green) and anti-HA antibody to visualize *Eh*Rab11B (red). Bars, 10 μm.

the *Eh*Rab11B-overexpressing transformant is due to the activation of the default BFA-insensitive pathway or alternative BFA-sensitive pathway(s), zymograms of the BFA-treated and untreated transformants were compared (Fig. 4F and G). The zymogram did not change with BFA treatment in either the *Eh*Rab11B-overexpressing or control transformant, suggesting that activation of the default BFA-insensitive pathway is likely the reason for the observed phenotype. The transport of the putative fibronectin receptor, detected with the monoclonal antibody against the galactose/N-acetylgalactosamine-specific lectin intermediate subunit (Cheng *et al.*, 2001) was partially inhibited under the same conditions (data not shown).

### *Overexpression of EhRab11B increased both intracellular and secreted amounts of three major cysteine proteases*

To further examine the level of expression and secretion of individual cysteine proteases in the *Eh*Rab11B-overexpressing transformant, the relative amounts of three major cysteine proteases, i.e. CP1, CP2 and CP5, were determined by fluorometric estimation of immunoblots using specific antibodies raised against recombinant cysteine proteases (Sato *et al.*, 2006). These cysteine proteases were detected as a single 29-kDa band under reducing conditions (Fig. 5). We first verified the specificity (or cross-reactivity) of each antibody against the cysteine proteases (Fig. 5C). Despite high sequence homology among the three cysteine proteases (CP1 and CP2, 81%; CP1 and CP5, 51%; CP2 and CP5, 50%), anti-CP2 and anti-CP5 specifically reacted with the corresponding cysteine protease, while anti-CP1 antibody cross-reacted with CP2 with a similar efficiency to CP1. In the culture supernatant, the amount of CP1/CP2, CP2 and CP5, detected by anti-CP1, CP2 and CP5 antibody, respectively, increased by 18.0, 4.2 and 2.0-fold, respectively, in the *Eh*Rab11B-overexpressing transformant (Fig. 5B). Similarly, in the lysate, the amount increased by 6.6, 3.2 and 2.0-fold, respectively (Fig. 5A). These data were consistent with the results of cysteine protease activity described

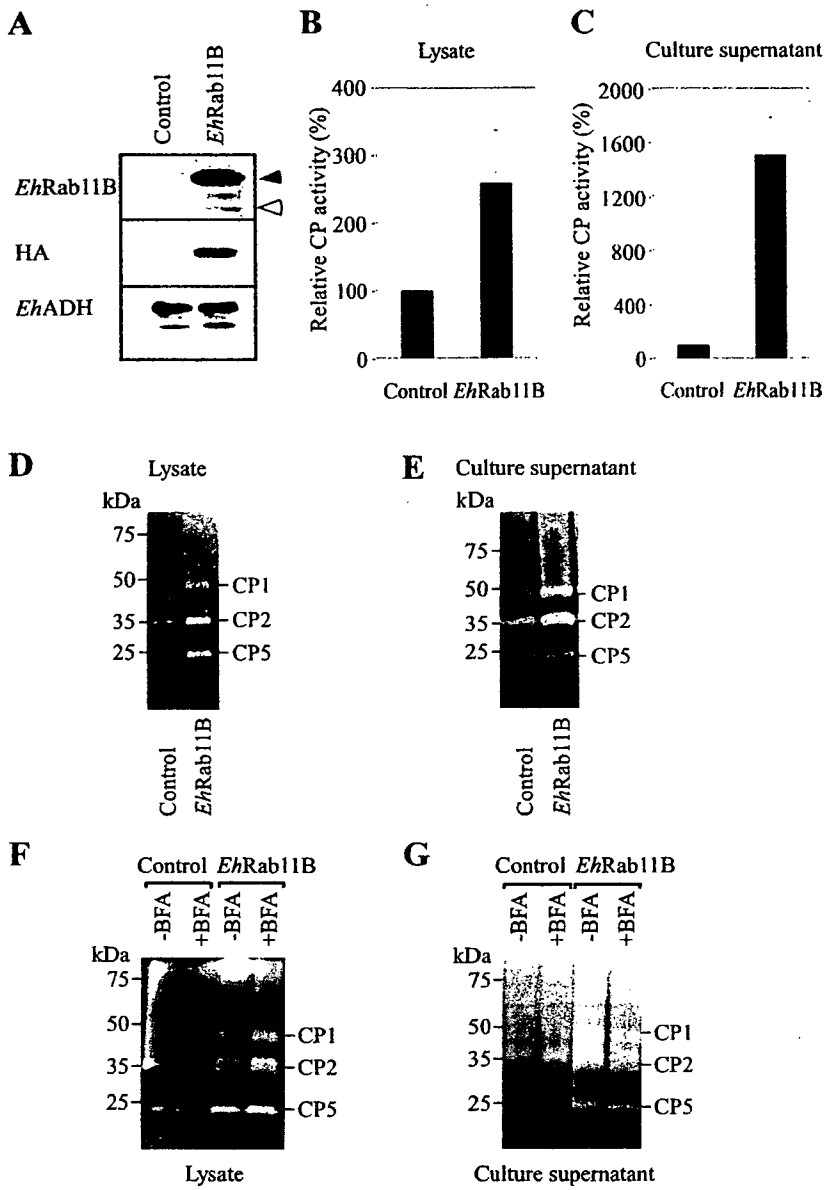


**Fig. 4.** Effects of *Eh*Rab11B overexpression on intracellular and secreted cysteine protease activity.
A. Overexpression of *Eh*Rab11B verified by immunoblotting using anti-HA and anti-*Eh*Rab11B antibodies. Approximately 20 μg of total lysate from the control or HA-*Eh*Rab11B-overexpressing transformant was electrophoresed on a SDS-polyacrylamide gel under reducing conditions and subjected to an immunoblot analysis using anti-*Eh*Rab11B, anti-HA and anti-*Eh*ADH (control). White and black arrow indicate endogenous and HA-tagged *Eh*Rab11B respectively.
B and C. The cysteine protease activity in the total lysate (B) and culture supernatant (C) of the transformants was measured using z-Arg-Arg-7-amino-4-trifluoromethylcoumarin as a substrate. The level of activity is shown as a percentage relative to the control transformant. Error bars represent SEs of three independent experiments.
D and E. Gelatin substrate gel electrophoresis. Approximately 1 μg of lysate (D) or 12 μl of culture supernatant (E) per lane was electrophoresed on a 12% SDS polyacrylamide gel copolymerized with 0.1% gelatin.
F and G. To evaluate the effect of BFA on cysteine protease activity, the transformants were pretreated with 200 μM of BFA for 2 h, and 4 μg of lysate (F) and 14 μl of crude culture supernatant (G) were subjected to gelatin substrate gel electrophoresis as in D and E.

above. That overexpression of *Eh*Rab11B increased the intracellular and secreted amounts of all three cysteine proteases suggests that *Eh*Rab11B is involved in the transport of these major cysteine proteases. To ensure cysteine protease production *per se* was not affected by *Eh*Rab11B overexpression, the steady-state amount of the mRNA of three major cysteine proteases (CP1, CP2 and CP5) as well as an irrelevant control enzyme, methionine γ-lyase 2, was measured by quantitative RT-PCR. The steady-state level of CP1, CP2 or CP5 mRNA, when normalized against methionine γ-lyase 2 mRNA, remained unchanged in the *Eh*Rab11B-overexpressing transformant compared with the control transformant (at 86%, 70% or 98% of the mRNA level of the control, respectively; $p > 0.05$; data not shown).

Finally, to exclude the possibility that the increased cysteine protease activity in the culture medium of the *Eh*Rab11B-overexpressing transformant is due to lysed cells, we measured alcohol dehydrogenase (ADH) activity in the culture supernatant and the cell lysate of the *Eh*Rab11B-overexpressing and control transformants. The ADH activity released into the culture medium by $2 \times 10^6$ *Eh*Rab11B-overexpressing and control transformant trophozoites for 1 h was $2.2 \times 10^{-3}$ and $1.2 \times 10^{-3}$ U per ml of culture supernatant, respectively, while the ADH activity in the lysate of these transformants was $1.17 \times 10^{-2}$ and $1.00 \times 10^{-2}$ U per mg protein respectively. Thus, the 15-fold increase in secreted cysteine protease activity observed for the *Eh*Rab11B-overexpressing transformant

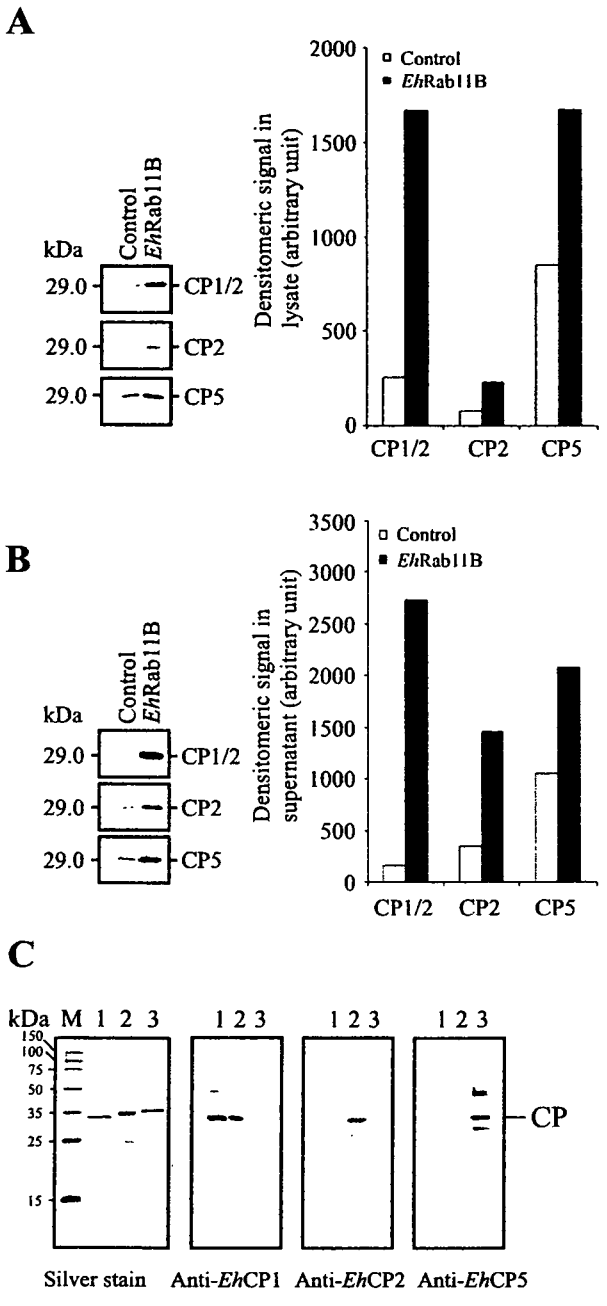


**Fig. 5.** Immunoblot analysis of intracellular and secreted CP1, CP2 and CP5.
A and B. Approximately 10 μg of total lysate (A) or 10 μl of concentrated culture supernatant (B) was electrophoresed on a 12% SDS-polyacrylamide gel, and subjected to an immunoblot assay with antibodies raised against recombinant *Eh*CP1, *Eh*CP2 and *Eh*CP5. The densitometric quantification of each cysteine protease, shown in the right panels (A and B), was performed by Quantity software version 4.2.1 and the level of cysteine proteases was expressed in arbitrary units.
C. Specificity and cross reactivity of cysteine protease antibodies. Approximately 150 ng of affinity-purified histidine-tagged recombinant CP1 (lane 1), CP2 (lane 2) or CP5 (lane 3) was electrophoresed and subjected to either silver staining (C, left panel) or an immunoblot assay using anti-*Eh*CP1, *Eh*CP2 and *Eh*CP5 antibodies.

was not attributable to a subtle increase in the lysis of this transformant.

### *EhRab11B-overexpressing trophozoites showed an augmented disruption of CHO monolayers*

It has been well established that both amoeba extracts and live trophozoites degrade monolayers of cultured mammalian cells (Hellberg *et al.*, 2001; Mitra *et al.*, 2005; 2006; Tillack *et al.*, 2006) and cysteine proteases are primarily responsible for this cytopathic effect (Reed *et al.*, 1993). We examined whether the increased secretion of cysteine proteases caused by the overexpression of *Eh*Rab11B influences the destruction of CHO monolayers (Fig. 6A). The *Eh*Rab11B-overexpressing transformant killed CHO cells more efficiently than the control transformant. For example, the *Eh*Rab11B-overexpressing transformant destroyed 81.0 ± 8.0% CHO cells in 90 min, while the control transformant destroyed only 16.0 ± 3.7%. Preincubation of *Eh*Rab11B-overexpressing and control transformants with 200 μM E64 for 60 min reduced the extent to which the CHO monolayer was destroyed by 70–75% (Fig. 6B), suggesting that in addition to cysteine proteases, other hydrolases are also involved in the destruction of CHO cells, which is consistent with previous results (Hellberg *et al.*, 2001).

### *Overexpression of* Eh*Rab11B enhanced the release of a fluid-phase marker*

As Rab11 has been implicated in the recycling of endosomes in yeast and mammals (Benli *et al.*, 1996; Ullrich *et al.*, 1996; Ren *et al.*, 1998), effects of the overexpression of *Eh*Rab11B on the exocytosis of an incorporated fluid-phase marker were investigated. We measured the release of the pH-insensitive fluid-phase marker RITC-dextran by monitoring the decrease in the intracellular RITC fluorescence of transformants preloaded with RITC-dextran and cultured in a marker-free medium. The release of the fluid-phase marker was 1.5–2.0-fold faster in the *Eh*Rab11B-overexpressing transformant than the control transformant (Fig. 7). The magnitude of the enhancement of exocytosis of the fluid-phase marker by *Eh*Rab11B overexpression was much lower than that of the oversecretion of cysteine proteases. This agrees well with limited cross-talk between the endocytic pathway and *Eh*Rab11B, which was demonstrated by the partial colocalization of dextran/*Eh*Rab11B during endocytosis (Fig. 2).

## Discussion

In the present study, we have demonstrated for the first time that one of the four Rab11 isotypes plays a crucial role in virulence, in particular the regulation of transport

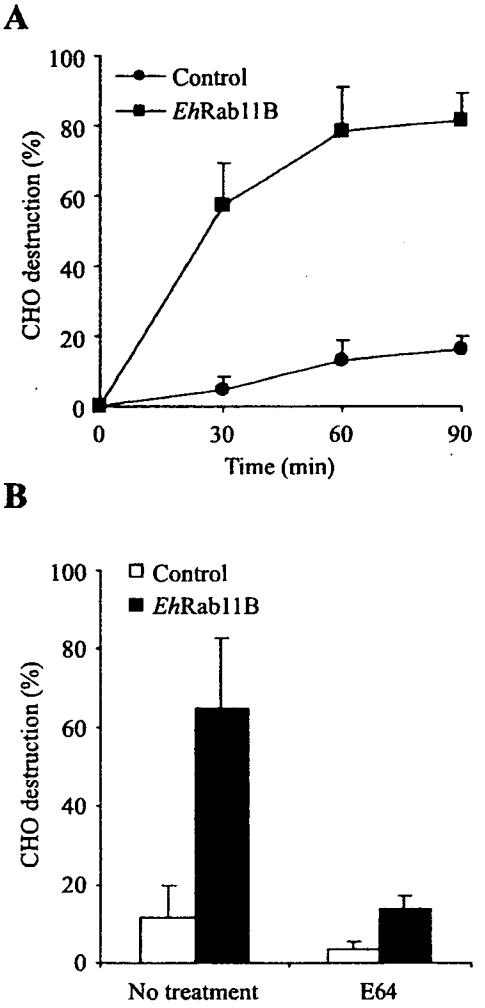


**Fig. 6.** Effects of *Eh*Rab11B-overexpression on the destruction of CHO monolayers.
A. Kinetics of CHO cell killing by the *Eh*Rab11B-overexpressing and control transformants. Approximately $1.5 \times 10^5$ trophozoites of the *Eh*Rab11B-overexpressing and control transformants were added to a monolayer of CHO cells and incubated at 35°C for the period indicated.
B. Effects of E64 on CHO cell killing. The *Eh*Rab11B-overexpressing and control transformants were pretreated with 200 μM of E64 for 2 h and incubated with CHO cells for 60 min. Monolayer destruction is expressed as the percentage of destroyed cells. Data shown here are the mean and standard deviation of three independent experiments.

and secretion of a well-established virulence factor, in enteric protozoan parasites. We have shown that overexpression of *Eh*Rab11B caused a dramatic increase in secreted as well as, to a lesser degree, intracellular cysteine protease activity, and thereby enhanced *in vitro* cytolytic activity.

Although Rab11 has been implicated in the secretion of several essential cellular factors, the present study is the first to show that Rab11 is directly involved in the pathogenesis of protozoan parasites. It was previously shown that Rab11 acts as a component of the exocytic machinery in $Ca^{2+}$-triggered and constitutive secretion in neuroendocrine and non-neuronal cells (Khvotchev *et al.*, 2003). In mammalian adipocytes, Rab11, together with Arf6, plays a crucial role in the constitutive and insulin-stimulated secretion of one of the adipokines, ACRP30 (Clarke *et al.*, 2006), suggesting that the recycling of endosomes via Rab11 plays an important role in this process. It has also recently been shown that dual Rab11/Arf-binding proteins, FIP3 and 4, function in the delivery of the recycling endosomes to the site of cleavage (cleavage furrow) during cytokinesis by coupling Rab11-positive vesicles from recycling endosomes with the cleavage furrow via interaction with Arf6 and the Exocyst (Fielding *et al.*, 2005).

We have previously shown that the transport and secretion of cysteine proteases are regulated through the specific interaction of *Eh*Rab7A with a novel effector called the retromer-like complex, composed of Vps26, Vps29 and Vps35 (Nakada-Tsukui *et al.*, 2005). Although the interaction of *Eh*Rab7A with the retromer-like complex is involved in part in the regulation of transport and secretion, the fold increase in intracellular and secreted levels of cysteine proteases caused by overexpression of *Eh*Rab7A is much less than that observed on overexpression of *Eh*Rab11B, shown in this study. These data suggest that *Eh*Rab11B plays a pivotal role in the trafficking of cysteine proteases. Alternatively, the remarkable changes in cysteine protease activity caused by *Eh*Rab11B overexpression might be attributable to the high level of overexpression of *Eh*Rab11B (ninefold), compared with only an approximately twofold increase in the case of overexpression of *Eh*Rab7A and *Eh*Rab5.

Although among the three cysteine proteases examined CP1 appeared to be influenced most dramatically by *Eh*Rab11B overexpression, *Eh*Rab11B mediates BFA-insensitive transport of all three major cysteine proteases and there is no stringent specificity in the *Eh*Rab11B-mediated pathway (Figs 3 and 4). It has recently been reported that overexpression of CP5 causes concomitant augmentation of the amount and activity of both CP1 and CP2 (Tillack *et al.*, 2006), which may suggest that CP5 is a key processing protease of other cysteine proteases. It is conceivable that similarly, activation of *Eh*Rab11B-mediated transport enhances the activity of a key processing enzyme, which in turn results in an augmented expression of various cysteine proteases. Although the pore-forming peptide amoebapore and the surface galactose/N-acetylgalactosamine-specific lectin were implicated in virulence *in vitro* and *in vivo* (Vines *et al.*, 1998; Leippe, 1999), it has not been shown in the present study if the transport and secretion of these proteins as well as other hydrolytic proteins are also mediated by *Eh*Rab11B. However, it is unlikely that *Eh*Rab11B mediates the transport of plasma membrane proteins because

the *Eh*Rab11B-mediated transport pathway is resistant to BFA while the galactose/N-acetylgalactosamine-specific lectin was shown to be transported via the 'classical' BFA-sensitive pathway (Manning-Cela *et al.*, 2003). It needs to be determined if other secreted virulence factors including amoebapore are also transported via an *Eh*Rab11B-associated pathway. In mammalian cells, GBF1, an Arf guanine-nucleotide exchange factor (GEF), was shown to be resistant to BFA and displayed specificity for Arf5, not but Arf1, the latter of which was catalysed by BFA-sensitive Arf GEF (Claude *et al.*, 1999). *E. histolytica* encodes 10 Arf proteins (Clark *et al.*, 2007) and nine Arf GEF-like proteins (Y. Saito-Nakano and T. Nozaki, unpublished), which raises the possibility that sensitivity to BFA may vary among these Arf-GEFs and the secretion of cysteine proteases is regulated by a pathway involving a BFA-insensitive Arf-GEF in *E. histolytica*.

The simultaneous increase of cysteine protease activity in both the whole lysate and the culture medium caused by *Eh*Rab11B overexpression has not been well explained. There are at least a few possible explanations. First, cysteine proteases that are usually destined to be transported to the degradation compartment were redirected to be accumulated in the storage compartment and also trafficked via the secretory pathway. This may be a consequence of either the ablation or enhancement of post-translational modifications by *Eh*Rab11B overexpression. Second, overexpression of *Eh*Rab11B activated an unidentified key protease responsible for the processing and activation of various cysteine proteases. It needs to be carefully examined if the simple overexpression of individual cysteine proteases increases secreted as well as intracellular amounts of cysteine proteases. It was previously shown that overexpression of three cysteine proteases, CP1, CP2 and CP5, caused a three- to sixfold increase in the total (i.e. intracellular) amount of cysteine proteases (Hellberg *et al.*, 2001; Tillack *et al.*, 2006). In the latter study, it was also shown that overexpression of CP1 or CP2 increased only the activity of a corresponding cysteine protease while overexpression of CP5 increased that of all three cysteine proteases. This observation may be causally connected with the finding that overexpression of CP1 or CP2 caused only a slight (1.5- to twofold) increase in the destruction of CHO cells whereas overexpression of CP5 augmented the killing by fivefold. However, it was not demonstrated in these studies whether overexpression of cysteine proteases also specifically or non-specifically increased the secretion of cysteine proteases.

A line of evidence suggested that *Eh*Rab11B is localized to the TGN and/or the post-Golgi compartments that interact with the endocytic pathway. *Eh*Rab11B partially colocalized with late endosomes (Fig. 2). In addition, the overexpression of *Eh*Rab11B dramatically activated the trafficking and secretion of cysteine proteases (Figs 3 and 4), and also slightly enhanced the exocytosis of the internalized fluid-phase marker (Fig. 7). These results also indicate that *Eh*Rab11B may control trafficking at the intersection of endocytic and secretory pathways in this organism. In contrast to *Eh*Rab11B, *Eh*Rab11A is not likely involved in endocytosis. Although *Eh*Rab11A was concentrated in the early and late endosome-enriched fractions (Temesvari *et al.*, 1999), *Eh*Rab11A was not colocalized with markers for fluid-phase and receptor-mediated endocytosis (McGugan and Temesvari, 2003). Recently, *Eh*Rab11A was shown to be translocated to the periphery of the cell under iron and serum starvation and during encystation, suggestive of its possible involvement in the secretory pathway under stress and during differentiation (Manning-Cela *et al.*, 2003). Therefore, we propose that *Eh*Rab11A and *Eh*Rab11B have distinct non-redundant functions, which need to be unequivocally demonstrated. Finally, considering that most organelles in *E. histolytica* are not morphologically discernible, 'classical' structures (Martinez-Palomo, 1986; Mazzuco *et al.*, 1997), the present study describing the unique involvement of Rab11 in the pathogenicity of this organism might illuminate the functional divergence of the secretory pathways in eukaryotes.

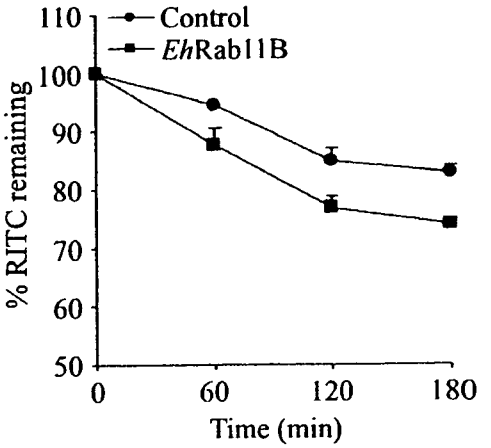


**Fig. 7.** Overexpression of *Eh*Rab11B affected exocytosis of the fluid-phase marker. The *Eh*Rab11B-overexpressing and control transformants were labelled with the fluid-phase marker RITC-dextran for 3 h, and chased for 180 min. At the time indicated, cells were collected and washed, and the fluorescence of RITC-dextran was measured using a fluorometer. The remaining fluorescence is shown as a percentage relative to the no-chase control.

## Experimental procedures

### *Chemical and reagents*

All chemicals of analytical grade were purchased from Wako (Tokyo, Japan) unless otherwise stated. Trans-epoxysuccinyl-L-leucylamido-(4-guanidino) butane (E64) was obtained from

Sigma-Aldrich (Tokyo, Japan). 2′,7′-bis(2-carboxyethyl)-5(6)-carboxyfluorescein acetoxymethyl ester, BFA, CellTracker Blue (7-amino-4-chloromethylcoumarin), LysoTracker Green DND 26, and LysoTracker Red DND-99 were purchased from Invitrogen (Carlsbad, CA).

### *Organisms and culture*

Trophozoites of *E. histolytica* strain HM-1:IMSS cl-6 were cultured axenically at 35°C in 13 × 100 mm screw-capped Pyrex glass tubes or plastic culture flasks in BI-S-33 medium as previously described (Diamond *et al.*, 1972; 1978). For the detection of proteins in the lysates and culture supernatant, approximately $1 \times 10^6$ trophozoites of the late-logarithmic growth phase were cultivated in 1 ml of serum-free BI-S-33 medium under anaerobic conditions using Anaerocult A (Merck, Darmstadt, Germany) on a 6-well culture plate (Corning, NY) at 35°C for 2 h. CHO cells were grown in F-12 medium (Invitrogen-Gibco, Grand Island, NY) supplemented with 10% fetal bovine serum on a 10-cm-diameter tissue culture dish (IWAKI, Tokyo, Japan) under 5% $CO_2$ at 37°C.

### *Quantitative RT-PCR*

Poly-A RNA was extracted from HM1: IMSS cl6 trophozoites with a Messenger RNA Isolation Kit (Stratagene), and treated with deoxyribonuclease I (Invitrogen) to exclude genomic DNA. Poly-A RNA was reverse transcribed with the SuperScript III First-Strand Synthesis System and oligo$(dT)_{20}$ primer (Invitrogen). PCR was performed with the resulting cDNA as a template and specific oligonucleotide primers using the ABI PRISM 7700 Sequence Detection System (Applied Biosystems, Japan). Primers used were 5′-GTT ATT ACA AAA GAA GCA GAA-3′ and 5′-TCA GCA ACA ACC TTT TTT GTT CTC-3′ (*Eh*Rab5); 5′-GCT GAA CAA TGG TGT TCA GAA CAT-3′ and 5′-TCA ACA AGG GCA ATC AGA CTT TTG-3′ (*Eh*Rab7A); 5′-TGT CAA AAA CAA AAT CTC TTT TTC-3′ and 5′-TTA GCA ACA TCC TCC TTT ATT TTC-3′ (*Eh*Rab11A); 5′-AAT AAT GCA TTC TTT TTT GAA ACA-3′ and 5′-TTA ACA ACA TTT CTT TTC TTC TGG-3′ (*Eh*Rab11B); 5′-TTC TTT ATT GAA ACT TCT GCT TTA-3′ and 5′-AAT ACA GCA CTT CTT ACC ACC TTG-3′ (*Eh*Rab11C); 5′-TTC TTT TTT GAA ACA TCA GCT TTT-3′ and 5′-TTA ACA AGC ACA ACC ACT TTT TTT-3′ (*Eh*Rab11D); 5′-CAA TGC AAG AAT AAC TAT TTT GCA-3′ and 5′-TCA GAG ATA TTC AAC ACC AGT TGG-3′ (CP1); 5′-AAA TGC AAG AAT AAC TAC TTT GCT-3′ and 5′-TCA AAG ATA TTG AAC GCC AGT TGG-3′ (CP2); 5′-AAA GAA TGT TCA TCA ACT CAG CTT-3′ and 5′-TTA AGC ATC AGC AAC CCC AAC TGG-3′ (CP5); and 5′-CAT GTT AAA TTA TGT GGA TTA GCT-3′ and 5′-TCA ATT ATT TTC TGA CCC GTC TTC-3′ (methionine γ-lyase 2); 5′-GAT CCA ACA TAT CCT AAA ACA ACA-3′ and 5′-TCA ATT ATT TTC TGA CCC GTC TTC-3′ (RNA polymerase II 15 kDa subunit). Parameters for PCR were: an initial step of denaturation at 95°C for 9 min followed by 40 cycles of denaturation at 94°C for 30 s, annealing at 50°C for 30 s and extension at 65°C for 1 min. A final step at 95°C for 9 s, 60°C for 9 s and 95°C for 9 s was used to remove primer dimers.

### *Production of* E. histolytica *transformants overexpressing* Eh*Rab11B*

The *Eh*Rab11B protein coding region was amplified by PCR from cDNA using sense and antisense oligonucleotides containing appropriate restriction sites at the 5′-end, 5′-GA AGATCT A ATG GCTAGC GGA TCA GAA GAA TAT GAT TTC-3′ and 5′-CCA CTCGAG TTA ACA ACA TTT CTT TTC TTC TGG-3′ (restriction sites are underlined). A sequence tag consisting of three tandem repeats of the haemagglutinin (HA) peptide was inserted at the amino terminus together with an engineered NheI site (Saito-Nakano *et al.*, 2004). A PCR-amplified DNA fragment was digested with BglII and XhoI, and ligated into BglII and XhoI sites of the expression vector pEhEx, to produce pH 11B. The wild-type trophozoites were transformed with either pH 11B or pEhEx by liposome-mediated transfection as previously described (Nozaki *et al.*, 1999).

### *Assay for destruction of CHO monolayers*

The destruction of CHO monolayers was quantified as described previously with slight modifications (Mitra *et al.*, 2006). Briefly, CHO cells were labelled with 40 μM of CellTracker Blue in the growth medium at 37°C for 2 h, and then washed and chased in the growth medium for 2 h. After the medium was replaced with prewarmed OPTI-MEM (Invitrogen-Gibco) supplemented with 137 mM L-cysteine and 19 mM ascorbic acid, pH 6.7, approximately $1.5 \times 10^5$ *E. histolytica* trophozoites were added and incubated at 35°C for 0, 30, 60 and 90 min. After this incubation, the remaining CHO cells were collected using trypsin and the fluorescence of CellTracker blue was measured using a fluorometer (F-2500, Hitachi, Japan) with excitation and emission at 353 and 465 nm respectively. The number of adherent CHO cells was proportional to the intensity of CellTracker blue staining and expressed as a percentage of the remaining fluorescence of untreated CHO cells.

### *Preparation of cell lysates and culture supernatants*

A semi-confluent culture was harvested at 48–72 h after initiation of the culture and suspended in the serum-free BI-S-33 medium at $1 \times 10^6$ cells $ml^{-1}$. After the culture was incubated at 35°C for 2 h, the culture supernatant was centrifuged at 15 000 *g* for 10 min at 4°C. Attached trophozoites were washed with ice-cold phosphate-buffered saline (PBS) containing 2% glucose and collected by centrifugation at 1000 *g* for 10 min. For immunoblot analysis, the culture supernatant was concentrated by 10-fold with TCA-acetone precipitation. For soluble extracts, approximately $2.5 \times 10^5$ trophozoites lysed in 100 μl of PBS by three cycles of freeze–thawing were centrifuged at 14 000 *g* for 15 min at 4°C, and the supernatant was saved.

### *Assay for cysteine protease activity*

Cysteine protease activity was measured with the cleavage of the synthetic peptide substrate z-Arg-Arg-7-amino-4-trifluoromethylcoumarin (ICN, Aurora, OH) monitored by a spectrophotometric method as described previously (Nowak *et al.*, 2004; Nakada-Tsukui *et al.*, 2005). The activities were expressed in mmol of z-Arg-Arg-7-amino-4-trifluoromethylcoumarin produced per milligram of lysate protein. The statistical significance of the data was evaluated with Student's *t*-test.

### *Assay for ADH activity*

The ADH activity in the cell lysate and the culture supernatant was determined by monitoring the increase in absorbance at

334 nm due to the reduction of $NADP^+$ with a spectrophotometer (Ultraspec 3000, Pharmacia Biotech) in 200 µl of 50 mM glycine-NaOH (pH 9.5) containing 250 µM NADP+ and 125 mM ethanol at 35.5°C for 1 h, essentially as described (Kumar *et al.*, 1992). Approximately $5 \times 10^5$ trophozoites were incubated in 250 µl of OPTI-MEM (see above) at 37°C for 1 h. One unit of activity was defined as the amount of enzyme that produced 1 µmol of NADPH per min at 35.5°C.

### *Substrate gel electrophoresis*

Protease activity was assayed by gelatin substrate gel electrophoresis as described previously (Reed *et al.*, 1989; Hellberg *et al.*, 2000). Briefly, 12 µl of the crude culture supernatant or 1–4 µg of the lysate was electrophoresed under non-reducing conditions on a 12% SDS-polyacrylamide gel copolymerized with 0.1% gelatin (Sigma-Aldrich, Japan). After separation, the gel was washed with 2.5% Triton X-100 to remove SDS for 1 h, rinsed twice with distilled water, and incubated in the developing buffer (100 mM Sodium acetate, 1% Triton X-100, 2 mM DTT) at room temperature for 3 h. After staining and several cycles of destaining, protease activity was detected by the degradation of gelatin, indicated by a clear band on the Coomassie brilliant blue-stained background. Molecular weight was estimated from the migration of standards (Bio-Rad Laboratories, Richmond, CA).

### *Production and purification of recombinant cysteine proteases*

*EhCP1*, *EhCP2* and *EhCP5* genes lacking putative signal sequences were amplified by PCR using trophozoite cDNA as a template and oligonucleotide primers designed based on available nucleotide sequences: Q01957 (CP1), Q01958 (CP2) and AAFB01000593 (CP5). PCR products were inserted into the pET-15b expression plasmid (Novagen). Histidine-tagged recombinant cysteine proteases were produced as inclusion bodies in *E. coli* strain BL21 (DE3). Recombinant cysteine proteases were purified by affinity chromatography under denaturing conditions. Refolding and activation were performed as previously described (Hellberg *et al.*, 2002; Sato *et al.*, 2006) with some modifications. Briefly, recombinant CP1 and CP2 (100 µg $ml^{-1}$, 30–40 µl) were dialysed against refolding buffer B (100 mM Tris-HCl, pH 8.8, 300 mM NaCl, 5% glycerol, 0.1 mM EDTA, 3 mM reduced glutathione and 0.5 mM oxidized glutathione) at 4°C for 1.5 h, and subsequently against refolding buffer C (25 mM Tris-HCl, pH 6.8 and 150 mM NaCl) at 4°C for 1.5 h. Recombinant CP5 was treated similarly except that refolding buffer B contained 50 mM Tris-HCl, pH 8.8 and refolding buffer C contained 50 mM Tris-HCl, pH 6.8 and no NaCl. The refolded recombinant cysteine proteases were activated by incubation with an equal volume of 100 mM Tris-HCl, pH 8.8, 20 mM DTT and 2% Triton X-100 at 37°C for 30 min.

### *Antibodies*

Affinity-purified anti-*Eh*CP1, anti-*Eh*CP2, anti-*Eh*CP5 and anti-*Eh*Rab11B rabbit polyclonal antibodies were commercially produced at Kitayama-Rabes (Nagano, Japan). Anti-HA 16B12 mouse monoclonal antibody was purchased from Berkeley Antibody (Berkeley, CA). Anti-*Eh*ADH rabbit polyclonal antibody was described previously (Sanuki *et al.*, 2001). Anti-*Eh*Sec61 α-subunit and anti-DPMS rabbit polyclonal antibodies were a gift from Rosana Sánchez-López. Alexa Fluor anti-mouse and anti-rabbit IgG, and horseradish peroxidase (HRP)-conjugated goat anti-mouse and anti-rabbit IgG were purchased from Invitrogen (Carlsbad, CA).

### *Immunoblot analysis*

Cell lysates and culture supernatants were separated on 12% (w/v) SDS-polyacrylamide gels and subsequently electrotransferred onto nitrocellulose membranes (Hybond-C Extra; Amersham Biosciences UK, Little Chalfont, Bucks, UK) essentially as described (Tokoro *et al.*, 2003). Non-specific binding was blocked by incubating the membranes for 1.5 h at room temperature in 5% non-fat dried milk in TBST (50 mM Tris-HCl, pH 8.0, 150 mM NaCl and 0.05% Tween-20). The blots were reacted with primary antibodies specific for *Eh*CP1, *Eh*CP2, *Eh*CP5, *Eh*Rab11B, *Eh*ADH (control) and HA 16B12 at a dilution of 1:40 to 1:1000. The membranes were washed with TBST and further reacted with HRP-conjugated anti-rabbit or anti-mouse IgG antisera (1:10 000–1:20 000) at room temperature for 1.5 h. After further washing with TBST, specific proteins were visualized with chemiluminescence detection (Millipore Corporation, Billerica, MA). Densitometric measurements were performed using Quantity One software (version 4.2.1, Bio-Rad Laboratories, Hercules, CA).

### *Indirect immunofluorescence*

The trophozoites were incubated with 2 mg $ml^{-1}$ of FITC-dextran in BI-S-33 medium for 1 h, washed, and further incubated in fresh prewarmed BI-S-33 medium for specific periods (0, 30, 60 and 120 min). Cells were transferred to 8-mm round wells on a slide glass, fixed with 3.7% paraformaldehyde, and permeabilized with 50 mM digitonin/PBS as previously described (Saito-Nakano *et al.*, 2004). The cells were then reacted with anti-HA 16B12 mouse monoclonal antibody (1:1000) and Alexa Fluor-568 anti-mouse secondary antibody (1:1000). To examine the subcellular localization of *Eh*Rab11B in ER, anti-*Eh*Sec61 α-subunit or anti-*Eh*DPMS antibody (1:1000) was used. The samples were examined on a Carl-Zeiss LSM510 confocal laser-scanning microscope (Thornwood, NY). Images were further analysed using LSM510 software.

### *Measurement of fluid-phase exocytosis*

To measure fluid-phase exocytosis, $5 \times 10^5$ amoebic transformants were cultured in BI-S-33 medium containing the pH-insensitive fluorescent fluid-phase marker RITC-dextran (2 mg $ml^{-1}$; Mr = 70 000; Sigma-Aldrich, Japan) at 35°C for 3 h to saturate all endocytic compartments with the marker. The labelled cells were collected, washed and resuspended in warm marker-free BI-S-33 medium, and incubated at 35°C for 3 h. At specific time points (0, 60, 120 and 180 min), cells were collected and washed three times with ice-cold PBS. The cell pellets were then suspended in 300 µl of 50 mM Tris-HCl, pH 7.0 containing 1% Triton-X100 and vortexed for 15 s. Fluorescence intensity was measured using fluorometer (F-2500, Hitachi, Japan) at excitation and emission wavelengths of 570 and 610 nm respectively.

## Acknowledgements

The authors thank Rosana Sánchez-López for anti-*Eh*Sec61 α-subunit and anti-*Eh*DPMS antibodies, and Hiroshi Tachibana for anti-Igl antibody, as well as Vahab Ali, Mami Okada and Yoko Yamada for technical assistance and discussions. This work was supported in part by Grants-in-Aid for Scientific Research from the Ministry of Education, Culture, Sports, Science and Technology of Japan (17390124, 17790282, 18050006, 18073001), a grant for Research on Emerging and Re-emerging Infectious Diseases from the Ministry of Health, Labour and Welfare (01712004) and a grant for the Project to Promote the Development of Anti-AIDS Pharmaceuticals from the Japan Health Sciences Foundation (KA11501) to T.N.

## References

Ankri, S., Stolarsky, T., Bracha, R., Padilla-Vaca, F., and Mirelman, D. (1999) Antisense inhibition of expression of cysteine proteinases affects *Entamoeba histolytica*-induced formation of liver abscess in hamsters. *Infect Immun* **67:** 421–422.

Benli, M., Doring, F., Robinson, D.G., Yang, X., and Gallwitz, D. (1996) Two GTPase isoforms, Ypt31p and Ypt32p, are essential for Golgi function in yeast. *EMBO J* **15:** 6460–6475.

Bock, J.B., Matern, H.T., Peden, A.A., and Scheller, R.H. (2001) A genomic perspective on membrane compartment organization. *Nature* **409:** 839–841.

Bruchhaus, I., Jacobs, T., Leippe, M., and Tannich, E. (1996) *Entamoeba histolytica* and *Entamoeba dispar*: differences in numbers and expression of cysteine proteinase genes. *Mol Microbiol* **22:** 255–263.

Chavrier, P., and Goud, B. (1999) The role of ARF and Rab GTPases in membrane transport. *Curr Opin Cell Biol* **11:** 466–475.

Chen, Y.A., Scales, S.J., Patel, S.M., Doung, Y.C., and Scheller, R.H. (1999) SNARE complex formation is triggered by Ca2+ and drives membrane fusion. *Cell* **97:** 165–174.

Cheng, X.J., Hughes, M.A., Huston, C.D., Loftus, B., Gilchrist, C.A., Lockhart, L.A., *et al.* (2001) Intermediate subunit of the Gal/GalNAc lectin of *Entamoeba histolytica* is a member of a gene family containing multiple CXXC sequence motifs. *Infect Immun* **69:** 5892–5898.

Clark, C.G., Cecilia, U., Alsmark, M., Hofer, M., Saito-Nakano, Y., Ali, V., *et al.* (2007) Structure and content of the *Entamoeba histolytica* genome. *Adv Parasitol* (in press).

Clarke, M., Ewart, M.A., Santy, L.C., Prekeris, R., and Gould, G.W. (2006) ACRP30 is secreted from 3T3-L1 adipocytes via a Rab11-dependent pathway. *Biochem Biophys Res Commun* **342:** 1361–1367.

Claude, A., Zhao, B.P., Kuziemsky, C.E., Dahan, S., Berger, S.J., Yan, J.P., *et al.* (1999) GBF1: a novel Golgi-associated BFA-resistant guanine nucleotide exchange factor that displays specificity for ADP-ribosylation factor 5. *J Cell Biol* **146:** 71–84.

Diamond, L.S., Mattern, C.F., and Bartgis, I.L. (1972) Viruses of *Entamoeba histolytica*. I. Identification of transmissible virus-like agents. *J Virol* **9:** 326–341.

Diamond, L.S., Harlow, D.R., and Cunnick, C.C. (1978) A new medium for the axenic cultivation of *Entamoeba histolytica* and other *Entamoeba*. *Trans R Soc Trop Med Hyg* **72:** 431–432.

Eichinger, D. (1997) Encystation of *Entamoeba* parasites. *BioEssays* **19:** 633–639.

Fader, C.M., Savina, A., Sanchez, D., and Colombo, M.I. (2005) Exosome secretion and red cell maturation: exploring molecular components involved in the docking and fusion of multivesicular bodies in K562 cells. *Blood Cells Mol Dis* **35:** 153–157.

Fielding, A.B., Schonteich, E., Matheson, J., Wilson, G., Yu, X., Hickson, G.R., *et al.* (2005) Rab11-FIP3 and FIP4 interact with Arf6 and the exocyst to control membrane traffic in cytokinesis. *EMBO J* **24:** 3389–3399.

Goldenring, J.R., Soroka, C.J., Shen, K.R., Tang, L.H., Rodriguez, W., Vaughan, H.D., *et al.* (1994) Enrichment of rab11, a small GTP-binding protein, in gastric parietal cells. *Am J Physiol* **267:** G187–G194.

Harris, E., Yoshida, K., Cardelli, J., and Bush, J. (2001) Rab11-like GTPase associates with and regulates the structure and function of the contractile vacuole system in *Dictyostelium*. *J Cell Sci* **114:** 3035–3045.

Hellberg, A., Leippe, M., and Bruchhaus, I. (2000) Two major 'higher molecular mass proteinases' of *Entamoeba histolytica* are identified as cysteine proteinases 1 and 2. *Mol Biochem Parasitol* **105:** 305–309.

Hellberg, A., Nickel, R., Lotter, H., Tannich, E., and Bruchhaus, I. (2001) Overexpression of cysteine proteinase 2 in *Entamoeba histolytica* or *Entamoeba dispar* increases amoeba-induced monolayer destruction *in vitro* but does not augment amoebic liver abscess formation in gerbils. *Cell Microbiol* **3:** 13–20.

Hellberg, A., Nowak, N., Leippe, M., Tannich, E., and Bruchhaus, I. (2002) Recombinant expression and purification of an enzymatically active cysteine proteinase of the protozoan parasite *Entamoeba histolytica*. *Protein Expr Purif* **24:** 131–137.

Hume, A.N., Collinson, L.M., Rapak, A., Gomes, A.Q., Hopkins, C.R., and Seabra, M.C. (2001) Rab27a regulates the peripheral distribution of melanosomes in melanocytes. *J Cell Biol* **152:** 795–808.

Jacobs, T., Bruchhaus, I., Dandekar, T., Tannich, E., and Leippe, M. (1998) Isolation and molecular characterization of a surface-bound proteinase of *Entamoeba histolytica*. *Mol Microbiol* **27:** 269–6276.

Jeffries, T.R., Morgan, G.W., and Field, M.C. (2001) A developmentally regulated rab11 homologue in *Trypanosoma brucei* is involved in recycling processes. *J Cell Sci* **114:** 2617–2626.

Khvotchev, M.V., Ren, M., Takamori, S., Jahn, R., and Sudhof, T.C. (2003) Divergent functions of neuronal Rab11b in $Ca^{2+}$-regulated versus constitutive exocytosis. *J Neurosci* **23:** 10531–10539.

Kumar, A., Shen, P., Descoteaux, S., Pohl, J., Bailey, G., and Samuelson, J. (1992) Cloning and expression of an $NADP^{+}$-dependent alcohol dehydrogenase gene of *Entamoeba histolytica*. *Proc Natl Acad Sci USA* **89:** 10188–10192.

Lal, K., Field, M.C., Carlton, J.M., Warwicker, J., and Hirt, R.P. (2005) Identification of a very large Rab GTPase

family in the parasitic protozoan *Trichomonas vaginalis*. *Mol Biochem Parasitol* **143:** 226–235.

Leippe, M. (1999) Antimicrobial and cytolytic polypeptides of amoeboid protozoa-effector molecules of primitive phagocytes. *Dev Comp Immunol* **23:** 267–279.

Loftus, B., Anderson, I., Davies, R., Alismark, U.C.M., Samuelson, J., Amedeo, P., *et al.* (2005) The genome of the protist parasite *Entamoeba histolytica*. *Nature* **433:** 865–868.

McGugan, G.C., Jr and Temesvari, L.A. (2003) Characterization of a Rab11-like GTPase, EhRab11, of *Entamoeba histolytica*. *Mol Biochem Parasitol* **129:** 137–146.

McNiven, M.A., and Thompson, H.M. (2006) Vesicle formation at the plasma membrane and trans-Golgi network: the same but different. *Science* **313:** 1591–1594.

Manning-Cela, R., Marquez, C., Franco, E., Talamas-Rohana, P., and Meza, I. (2003) BFA-sensitive and insensitive exocytic pathways in *Entamoeba histolytica* trophozoites: their relationship to pathogenesis. *Cell Microbiol* **5:** 921–932.

Martinez-Palomo, A. (ed.) (1986) *The Biology of Entamoeba histolytica*, Chichester: Research Studies Press.

Mazzuco, A., Benchimol, M., and De Souza, W. (1997) Endoplasmic reticulum and Golgi-like elements in *Entamoeba*. *Micron* **28:** 241–247.

Mitra, B.N., Yasuda, T., Kobayashi, S., Saito-Nakano, Y., and Nozaki, T. (2005) Differences in morphology of phagosomes and kinetics of acidification and degradation in phagosomes between the pathogenic *Entamoeba histolytica* and the non-pathogenic *Entamoeba dispar*. *Cell Motil Cytoskeleton* **62:** 84–99.

Mitra, B.N., Kobayashi, S., Saito-Nakano, Y., and Nozaki, T. (2006) *Entamoeba histolytica*: differences in phagosome acidification and degradation between attenuated and virulent strains. *Exp Parasitol* **114:** 57–61.

Nakada-Tsukui, K., Saito-Nakano, Y., Ali, V., and Nozaki, T. (2005) A retromerlike complex is a novel Rab7 effector that is involved in the transport of the virulence factor cysteine protease in the enteric protozoan parasite *Entamoeba histolytica*. *Mol Biol Cell* **16:** 5294–5303.

Novick, P., and Zerial, M. (1997) The diversity of Rab proteins in vesicle transport. *Curr Opin Cell Biol* **9:** 496–504.

Nowak, N., Lotter, H., Tannich, E., and Bruchhaus, I. (2004) Resistance of *Entamoeba histolytica* to the cysteine proteinase inhibitor E64 is associated with secretion of proenzymes and reduced pathogenicity. *J Biol Chem* **279:** 38260–38266.

Nozaki, T., Asai, T., Sanchez, L.B., Kobayashi, S., Nakazawa, M., and Takeuchi, T. (1999) Characterization of the gene encoding serine acetyltransferase, a regulated enzyme of cysteine biosynthesis from the protist parasites *Entamoeba histolytica* and *Entamoeba dispar*. Regulation and possible function of the cysteine biosynthetic pathway in *Entamoeba*. *J Biol Chem* **274:** 32445–32452.

Que, X., and Reed, S.L. (2000) Cysteine proteinases and the pathogenesis of amebiasis. *Clin Microbiol Rev* **13:** 196–206.

Que, X., Brinen, L.S., Perkins, P., Herdman, S., Hirata, K., Torian, B.E., *et al.* (2002) Cysteine proteinases from distinct cellular compartments are recruited to phagocytic vesicles by *Entamoeba histolytica*. *Mol Biochem Parasitol* **119:** 23–32.

Reed, S., Bouvier, J., Pollack, A.S., Engel, J.C., Brown, M., Hirata, K., *et al.* (1993) Cloning of a virulence factor of *Entamoeba histolytica*. Pathogenic strains possess a unique cysteine proteinase gene. *J Clin Invest* **91:** 1532–1540.

Reed, S.L., Keene, W.E., and McKerrow, J.H. (1989) Thiol proteinase expression and pathogenicity of *Entamoeba histolytica*. *J Clin Microbiol* **27:** 2772–2777.

Ren, M., Xu, G., Zeng, J., De Lemos-Chiarandini, C., Adesnik, M., and Sabatini, D.D. (1998) Hydrolysis of GTP on rab11 is required for the direct delivery of transferrin from the pericentriolar recycling compartment to the cell surface but not from sorting endosomes. *Proc Natl Acad Sci USA* **95:** 6187–6192.

Saito-Nakano, Y., Nakazawa, M., Shigeta, Y., Takeuchi, T., and Nozaki, T. (2001) Identification and characterization of genes encoding novel Rab proteins from *Entamoeba histolytica*. *Mol Biochem Parasitol* **116:** 219–222.

Saito-Nakano, Y., Yasuda, T., Nakada-Tsukui, K., Leippe, M., and Nozaki, T. (2004) Rab5-associated vacuoles play a unique role in phagocytosis of the enteric protozoan parasite *Entamoeba histolytica*. *J Biol Chem* **279:** 49497–49507.

Saito-Nakano, Y., Loftus, B.J., Hall, N., and Nozaki, T. (2005) The diversity of Rab GTPases in *Entamoeba histolytica*. *Exp Parasitol* **110:** 244–252.

Saito-Nakano, Y., Mitra, B.N., Nakada-Tsukui, K., Sato, D., and Nozaki, T. (2007) Two Rab7 isotypes, *Eh*Rab7A and *Eh*Rab7B, play distinct roles in biogenesis of lysosomes and phagosomes in the enteric protozoan parasite *Entamoeba histolytica*. *Cell Microbiol* (in press).

Sanuki, J., Nakano, K., Tokoro, M., Nozaki, T., Okuzawa, E., Kobayashi, S., and Asai, T. (2001) Purification and identification of major soluble 40-kDa antigenic protein from *Entamoeba histolytica*: its application for serodiagnosis of asymptomatic amebiasis. *Parasitol Int* **50:** 73–80.

Saric, M., Vahrmann, A., Bruchhaus, I., Bakker-Grunwald, T., and Scholze, H. (2006) The second cysteine protease inhibitor, EhICP2, has a different localization in trophozoites of *Entamoeba histolytica* than EhICP1. *Parasitol Res* **100:** 171–174.

Sato, D., Nakada-Tsukui, K., Okada, M., and Nozaki, T. (2006) Two cysteine protease inhibitors, EhICP1 and 2, localized in distinct compartments, negatively regulate secretion in *Entamoeba histolytica*. *FEBS Lett* **580:** 5306–5312.

Savina, A., Vidal, M., and Colombo, M.I. (2002) The exosome pathway in K562 cells is regulated by Rab11. *J Cell Sci* **115:** 2505–2515.

Schluter, O.M., Khvotchev, M., Jahn, R., and Sudhof, T.C. (2002) Localization versus function of Rab3 proteins. Evidence for a common regulatory role in controlling fusion. *J Biol Chem* **277:** 40919–40929.

Seabra, M.C., Mules, E.H., and Hume, A.N. (2002) Rab GTPases, intracellular traffic and disease. *Trends Mol Med* **8:** 23–30.

Somsel Rodman, J., and Wandinger-Ness, A. (2000) Rab GTPases coordinate endocytosis. *J Cell Sci* **113:** 183–192.

Stanley, S.L., Jr, Zhang, T., Rubin, D., and Li, E. (1995) Role of the *Entamoeba histolytica* cysteine proteinase in amebic

 

liver abscess formation in severe combined immunodeficient mice. *Infect Immun* **63:** 1587–1590.

Stenmark, H., and Olkkonen, V.M. (2001) The Rab GTPase family. *Genome Biol* **2:** REVIEWS3007.

Stinchcombe, J.C., Barral, D.C., Mules, E.H., Booth, S., Hume, A.N., Machesky, L.M., *et al.* (2001) Rab27a is required for regulated secretion in cytotoxic T lymphocytes. *J Cell Biol* **152:** 825–834.

Temesvari, L.A., Harris, E.N., Stanley, S.L., Jr and Cardelli, J.A. (1999) Early and late endosomal compartments of *Entamoeba histolytica* are enriched in cysteine proteases, acid phosphatase and several Ras-related Rab GTPases. *Mol Biochem Parasitol* **103:** 225–241.

Tillack, M., Nowak, N., Lotter, H., Bracha, R., Mirelman, D., Tannich, E., and Bruchhaus, I. (2006) Increased expression of the major cysteine proteinases by stable episomal transfection underlines the important role of EhCP5 for the pathogenicity of *Entamoeba histolytica*. *Mol Biochem Parasitol* **149:** 58–64.

Tokoro, M., Asai, T., Kobayashi, S., Takeuhi, T., and Nozaki, T. (2003) Identification and characterization of two isoenzymes of methionine γ-lyase from *Entamoeba histolytica*: a key enzyme of sulfur-amino acid degradation in an anaerobic parasitic protist that lacks forward and reverse trans-sulfuration pathways. *J Biol Chem* **278:** 42717–42727.

Ullrich, O., Reinsch, S., Urbe, S., Zerial, M., and Parton, R.G. (1996) Rab11 regulates recycling through the peri-centriolar recycling endosome. *J Cell Biol* **135:** 913–924.

Urbe, S., Huber, L.A., Zerial, M., Tooze, S.A., and Parton, R.G. (1993) Rab11, a small GTPase associated with both constitutive and regulated secretory pathways in PC12 cells. *FEBS Lett* **334:** 175–182.

Vines, R.R., Ramakrishnan, G., Rogers, J.B., Lockhart, L.A., Mann, B.J., and Petri, W.A., Jr (1998) Regulation of adherence and virulence by the *Entamoeba histolytica* lectin cytoplasmic domain, which contains a β2 integrin motif. *Mol Biol Cell* **9:** 2069–2079.

Wilcke, M., Johannes, L., Galli, T., Mayau, V., Goud, B., and Salamero, J. (2000) Rab11 regulates the compartmentalization of early endosomes required for efficient transport from early endosomes to the trans-golgi network. *J Cell Biol* **151:** 1207–1220.

Willhoeft, U., Hamann, L., and Tannich, E. (1999) A DNA sequence corresponding to the gene encoding cysteine proteinase 5 in *Entamoeba histolytica* is present and positionally conserved but highly degenerated in *Entamoeba dispar*. *Infect Immun* **67:** 5925–5929.

Zerial, M., and McBride, H. (2001) Rab proteins as membrane organizers. *Nat Rev Mol Cell Biol* **2:** 107–117.

Zhang, Z., Wang, L., Seydel, K.B., Li, E., Ankri, S., Mirelman, D., and Stanley, S.L., Jr (2000) *Entamoeba histolytica* cysteine proteinases with interleukin-1 beta converting enzyme (ICE) activity cause intestinal inflammation and tissue damage in amoebiasis. *Mol Microbiol* **37:** 542–548.

 

Available online at www.sciencedirect.com
ScienceDirect
Molecular & Biochemical Parasitology 153 (2007) 107–114
MOLECULAR & BIOCHEMICAL PARASITOLOGY

# An *Entamoeba* sp. strain isolated from rhesus monkey is virulent but genetically different from *Entamoeba histolytica*☆

Hiroshi Tachibana[a,*], Tetsuo Yanagi[b], Kishor Pandey[b], Xun-Jia Cheng[a], Seiki Kobayashi[c], Jeevan B. Sherchand[d], Hiroji Kanbara[b]

[a] *Department of Infectious Diseases, Tokai University School of Medicine, Isehara, Kanagawa 259-1193, Japan*
[b] *Department of Protozoology, Institute of Tropical Medicine, Nagasaki University, Nagasaki 852-8523, Japan*
[c] *Department of Tropical Medicine and Parasitology, Keio University School of Medicine, Shinjuku-ku, Tokyo 160-8582, Japan*
[d] *Department of Microbiology and Parasitology, Infectious and Tropical Diseases Center, Tribhuvan University Teaching Hospital, Kathmandu, Nepal*

Received 2 December 2006; received in revised form 16 February 2007; accepted 22 February 2007
Available online 1 March 2007

**Abstract**

An *Entamoeba* sp. strain, P19-061405, was isolated from a rhesus monkey in Nepal and characterized genetically. The strain was initially identified as *Entamoeba histolytica* using PCR amplification of peroxiredoxin genes. However, sequence analysis of the 18S rRNA gene showed a 0.8% difference when compared to the reference *E. histolytica* HM-1:IMSS human strain. Differences were also observed in the 5.8S rRNA gene and the internal transcribed spacer (ITS) regions 1 and 2, and analysis of the serine-rich protein gene from the monkey strain showed unique codon usages compared to *E. histolytica* isolated from humans. The amino acid sequences of two hexokinases and two glucose phosphate isomerases also differed from those of *E. histolytica*. Isoenzyme analyses of these enzymes in the monkey strain showed different electrophoretic mobility patterns compared with *E. histolytica* isolates. Analysis of peroxiredoxin genes indicated the presence of at least seven different types of protein, none of which were identical to proteins in *E. histolytica*. When the trophozoites from the monkey strain were inoculated into the livers of hamsters, formation of amebic abscesses was observed 7 days after the injection. These results demonstrate that the strain is genetically different from *E. histolytica* and is virulent. Revival of the name *Entamoeba nuttalli* is proposed for the organism.


*Keywords:* *Entamoeba histolytica*; *Entamoeba nuttalli*; Rhesus monkey; rRNA gene; Virulency

## 1. Introduction

The enteric protozoan *Entamoeba histolytica* causes an estimated 50 million cases of amebic colitis and liver abscess in human, resulting in 100,000 deaths annually [1]. *Entamoeba dispar* is morphologically indistinguishable from *E. histolytica* but is nonpathogenic [2]. It has been reported that *E. histolytica/E. dispar* is commonly found in the feces of non-human primates, such as macaques and baboons [3–6]. Since *E. histolytica* infection in non-human primates is problematic not only for animal health but also as a possible source of transmission to humans, it is important to discriminate between *E. histolytica* and *E. dispar*. Recent studies have demonstrated that *E. dispar* infection is prevalent in captive and wild non-human primates, including baboons, macaques, and chimpanzees [7–11]. We have demonstrated that the prevalence of *E. dispar*, but not *E. histolytica*, is 43% in a wild colony of *Macaca fuscata fuscata* in Japan [10], 66% in captive *Macaca* monkeys [8], and 56% in captive chimpanzees [9]. In contrast, a limited number of *E. histolytica* infections in non-human primates have been confirmed [12–14]. However, it is unknown whether *E. histolytica* isolated from non-human primates is identical to that isolated from humans.

In the present study, we analyzed several genes of an *Entamoeba* strain isolated from a rhesus monkey, *Macaca mulatta*, and compared it with a reference strain isolated from humans.

*Abbreviations:* GPI, glucose phosphate isomerase; HXK, hexokinase; ITS, internal transcribed spacer; PAS, periodic acid-Schiff; PRX, peroxiredoxin

☆ *Note:* Nucleotide sequence data reported in this paper are available in the DDBJ, EMBL, and GenBank™ databases under the accession numbers AB282657 to AB282673.

* Corresponding author. Tel.: +81 463 93 1121; fax: +81 463 95 5450.
*E-mail address:* htachiba@is.icc.u-tokai.ac.jp (H. Tachibana).

0166-6851/$ – see front matter © 2007 Elsevier B.V. All rights reserved.
doi:10.1016/j.molbiopara.2007.02.006

We report here that the monkey strain is virulent but genetically different from *E. histolytica*.

## 2. Materials and methods

### 2.1. Isolation and culture conditions

A fecal sample containing *Entamoeba* cysts was obtained from a rhesus monkey in Pashupati Nath Temple, Kathmandu, Nepal on June 2005. The sample was suspended in water for 24 h to remove *Blastocystis* spp. and then cultured in modified Tanabe-Chiba medium, which consists of an agar slant and an upper liquid medium in a screw-cap test tube, at 37 °C. The slant contained 1% agar in Ringer's solution supplemented with 0.1% L-asparagine, and the liquid medium contained phosphate-buffered saline (pH 7.6) supplemented with one-eighth the volume of horse serum. A microspatula of rice powder was added before use. Grown trophozoites of the *Entamoeba*, designated as the P19-061405 strain, were brought to Japan and cultured in Robinson's medium at 37 °C [15]. The trophozoites were treated with a cocktail of antibiotics and then cultured monoxenically with live *Crithidia fasciculata* in BI-S-33 medium supplemented with 15% adult bovine serum at 37 °C [16]. The monoxenically cultured trophozoites were used in most experiments in the present study. Finally, trophozoites of the strain were cultured axenically in the BI-S-33 medium and then cloned by limiting dilution, followed by examination using microscopy. Trophozoites of *E. histolytica* strains HM-1:IMSS, HK-9, Rahman, and NOT-12 were cultured axenically in BI-S-33 medium and were used as reference strains. Trophozoites of the *E. histolytica* SAW1453 strain were cultured xenically in Robinson's medium. Trophozoites of the *E. dispar* SAW1734RclAR strain were grown monoxenically with sterilized *C. fasciculata* in YIGADHA-S medium supplemented with 15% adult bovine serum at 37 °C and were also used as a reference strain [17].

### 2.2. PCR amplification

Genomic DNA of trophozoites was isolated using a DNeasy tissue kit (Qiagen). The primers used for PCR amplification are listed in Table 1. PCR of peroxiredoxin (PRX) genes was performed to distinguish between *E. histolytiica* and *E. dispar*, as previously described [18]. Amplification of the serine-rich protein gene was performed essentially as reported by Ghosh et al. [19]. Ribosomal RNA genes, hexokinase (HXK) genes, glucose phosphate isomerase (GPI) genes, and full-length PRX genes were amplified 30 cycles using *Pyrobest* DNA polymerase (Takara). The PCR conditions were as follows: denaturation at 94 °C for 15 s (195 s in cycle 1), annealing at 60 °C (for ribosomal RNA genes), or 58 °C (for other genes) for 30 s, and extension at 72 °C for 120 s (600 s in cycle 30). The sizes of PCR products were confirmed by electrophoresis on agarose gels.

### 2.3. Sequencing

PCR products of the ribosomal RNA gene and serine-rich protein gene were purified using a QIAEX II gel extraction kit

Table 1
Primers used in this study

| Gene or protein (species) | Direction: Sequence (5′–3′) | GeneBank accession no. |
|---|---|---|
| PRX (Eh) | S (P11): GGA GGA GTA GGA AAG TTG AC<br>AS (P12): TTC TTG CAA TTC CTG CTT CGA | D10512 |
| PRX (Ed) | S (P13): AGG AGG AGT AGG AAA ATT AGG<br>AS (P14): TTC TTG AAA CTC CTG TTT CTA C | D00872 |
| Serine-rich protein (Eh) | S: GCT AGT CCT GAA AAG CTT GAA GAA GCT G<br>AS: GGA CTT GAT GCA GCA TCA AGG T | M80910 |
| rRNA (Eh) | S: GAA GAA GTC AAA AGT AGG AGA ATA AAG AAA GG<br>AS: CCC TTA TTG ATA TGC TTA AGT TAA GGG AGTC | X65163 |
| HXK (Eh)<br>HXK1<br>HXK2 | S: ATG CAA GAA ATC ATT GAT CAA TTT<br>AS: TTA GTG TTT ACA TGC AAC AGC A<br>AS: TTA TTG TTT GCA TGC AAC AGC A | X82197, X82198<br>X82197<br>X82198 |
| GPI (Eh) | S: ATG TTA CCA ACT CTT CCT GAA T<br>AS: TTA GTT TTT TCT CAT ATC TTT AAC A | AB217859 |
| PRX Full (Eh) | S: ATG TCT TGC AAT CAA CAA AAA GA<br>AS: TTA ATG TGC TGT TAA ATA TTT CTT AAT | X70996 |
| 18S rRNA (Eh) | S: GTT TTA TAC ATT TTG AAG ACT TTA TG<br>AS: CAG ATC TAG AAA CAA TGC TTC TCT | X65163 |
| 18S rRNA (Ed) | S: ATT TTA TAC ATT TTG AAG ACT TTA CAT T<br>AS: GAA CAA GGT AGT ATT GAT ATA CTT G | AB282661* |
| 18S rRNA (P19) | S: TTT TAT ACA TTT TGA AGA CTT TGC ATA<br>AS: AAG GTA ATA TTG ATA TAC TCA GAT TA | AB282657* |

Eh, *E. histolytica*; Ed, *E. dispar*; P19, *Entamoeba* sp. P19-061405 strain; S, Sense; AS, Anti-sense.
* Present study.

(Qiagen) and subjected to direct sequencing. Amplified genes for HXK, GPI, and PRX were cloned using a Zero Blunt TOPO PCR cloning kit for sequencing (Invitrogen). Eight clones each from the *HXK* and *GPI* genes and 12 clones from *PRX* genes were subjected to sequencing, which was performed with a BigDye Terminator v3.1 cycle sequencing kit (Applied Biosystems). The reactions were run on an ABI Prism 3100 genetic analyzer (Applied Biosystems). Sequence data were analyzed using Genetyx-Mac ver. 11 (Genetyx).

### 2.4. Sandwich ELISA

Approximately $10^3$ trophozoites cultured monoxenically with *C. fasciculata* in BI-S-33 medium were analyzed using an *E. histolytica* antigen detection kit (*E. HISTOLYTICA II*, Tech-Lab). The protocol for stool samples was also used for cultured samples.

### 2.5. Indirect immunofluorescence microscopy

The reactivity of the *E. histolytica*-specific monoclonal antibody 4G6 against PRX was examined by indirect immunofluorescence microscopy, as described previously, except that monoxenic trophozoites were fixed with 4% paraformaldehyde [12,20].

### 2.6. Zymodeme analysis

Isoenzyme analysis of *Entamoeba* trophozoites in starch gel was performed according to the method of Sargeaunt [21].

### 2.7. Hepatic inoculation

Five male Syrian hamsters of 8 weeks of age were used in the study. Three hamsters were anesthetized by intraperitoneal injection of pentobarbital and then $3 \times 10^5$ trophozoites cultured monoxenically with *C. fasciculata* were inoculated into the left lobe of the liver. Two control hamsters received inoculation of live *C. fasciculata*. The hamsters were sacrificed 7 days after inoculation to examine the formation of amebic liver abscesses. Liver tissues, including abscesses, were fixed with 4% paraformaldehyde in phosphate buffer and then embedded in paraffin. Thin sections were stained with hematoxylin and eosin, and with periodic acid-Schiff (PAS) reagent.

## 3. Results

### 3.1. Identification of the P19-061405 strain by conventional methods

Cysts of *Entamoeba* in fecal samples were morphologically identified as *E. histolytica*/*E. dispar*. After the sample was transferred to culture, the trophozoites grew well in Tanabe-Chiba medium and Robinson's medium under xenic conditions. PCR amplification analysis of *PRX* genes demonstrated that the isolate P19-061405 was *E. histolytica* (Fig. 1). The trophozoites were also successfully cultured in BI-S-33 medium with *C. fasciculata* at 37 °C. No morphological differences were evident under light microscopy in comparison with human isolates of *E. histolytica*. Analysis of cultured trophozoites with the *E. histolytica* antigen detection kit indicated a positive optical density. Trophozoites of the isolate were also reactive with the *E. histolytica*-specific monoclonal antibody 4G6.

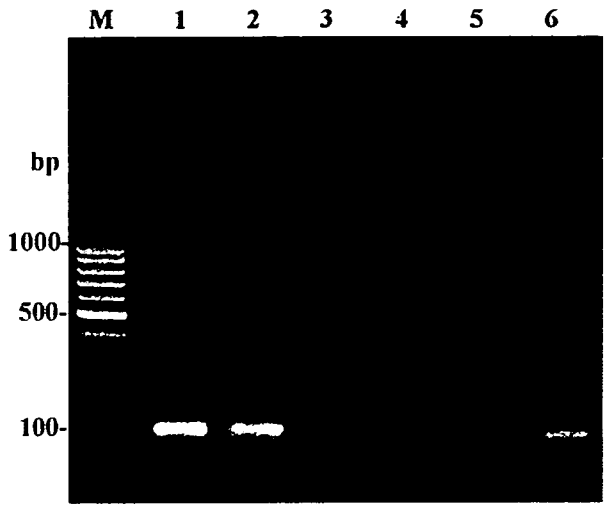


Fig. 1. PCR amplification of peroxiredoxin genes from trophozoites of the P19-061405 strain to distinguish between *E. histolytica* and *E. dispar*. Two sets of specific primers were used: P11 and P12 for *E. histolytica* (lanes 1–3) and P13 and P14 for *E. dispar* (lanes 4–6) [18]. Templates are genomic DNA from P19-061405 (lanes 1 and 4), *E. histolytica* HM-1:IMSS (lanes 2 and 5), and *E. dispar* SAW1734RclAR (lanes 3 and 6). M, DNA size marker (100 bp ladder).

### 3.2. Analysis of the ribosomal RNA gene

A region of ribosomal RNA genes of about 2.4 kb was amplified by PCR and sequenced directly. Sequence analysis of the 18S ribosomal RNA gene of the P19-061405 strain showed an identical size but a 0.8% (15/1945) difference in sequence, compared with the reported *E. histolytica* HM-1:IMSS strain (Fig. 2). On the other hand, the difference between P19-061405 and *E. dispar* SAW1734RclAR was 1.2% in the overlapping region. This difference is smaller than that the 1.5% difference between *E. histolytica* HM-1:IMSS and *E. dispar* SAW1734RclAR, indicating that the monkey strain is phylogenetically located between *E. histolytica* and *E. dispar*. Differences between the monkey strain and the human reference *E. histolytica* strain were also compared for the 5.8S ribosomal RNA gene and the internal transcribed spacer (ITS) 1 and 2 regions. One- and two-nucleotide differences were found in the 5.8S rRNA gene and ITS1 region, respectively. In the ITS2 region, a one-nucleotide insertion and a deletion of 5 nucleotides were observed in the monkey strain, in addition to substitution of 6 nucleotides. In other human *E. histolytica* strains, HK-9, Rahman, and NOT-12, no sequence differences were observed in the 2.4 kb region in comparison with the HM-1:IMSS strain. To confirm the sequence differences of the monkey strain from *E. histolytica* HM-1:IMSS and *E. dispar* SAW1734RclAR, PCR amplification of ribosomal RNA genes was performed using primers specific for each strain (Fig. 3). PCR products were detected only with

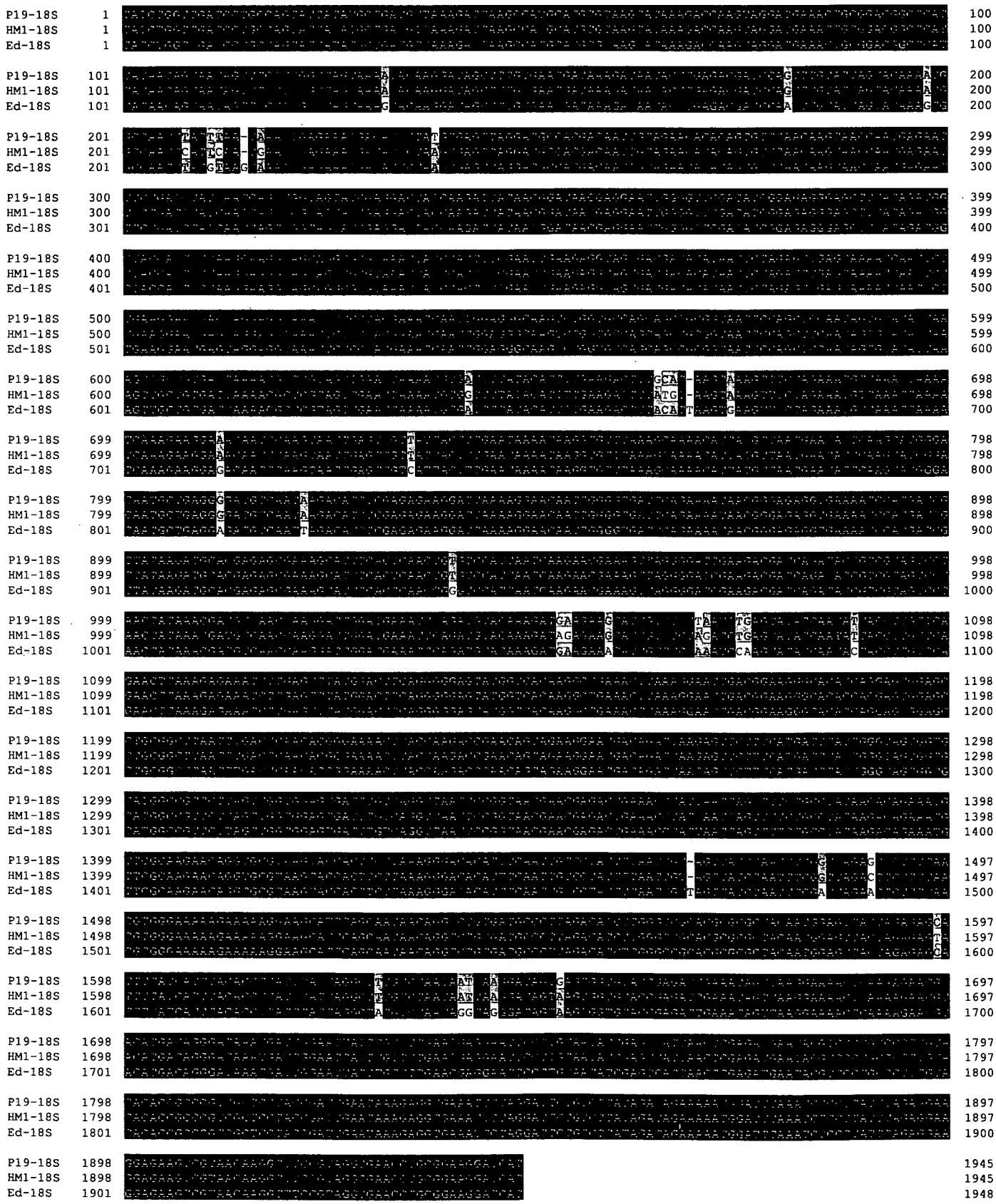


Fig. 2. Comparison of 18S ribosomal RNA genes from P19-061405 (top line), *E. histolytica* HM-1:IMSS (middle line, GenBank accession no. X65163), and *E. dispar* SAW1734RclAR (bottom line). Identical and conserved nucleotide sequences are highlighted in black and gray, respectively.

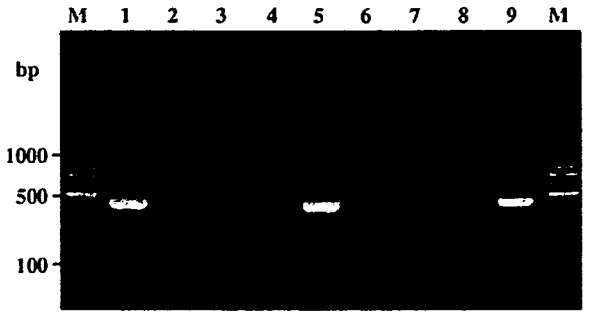


Fig. 3. PCR amplification of rRNA genes from trophozoites of P19-061405 strain, *E. histolytica*, and *E. dispar*. Three sets of primers specific for the P19-061405 strain (lanes 1–3), *E. histolytica* (lanes 4–6), and *E. dispar* (lanes 7–9) were used. Templates are genomic DNA from P19-061405 (lanes 1, 4, and 7), *E. histolytica* HM-1:IMSS (lanes 2, 5, and 8), and *E. dispar* SAW1734RclAR (lanes 3, 6, and 9). M, DNA size marker (100 bp ladder).

specific primers, indicating that the sequences of ribosomal RNA genes were clearly different among the three strains and that no contamination of *E. histolytica*/*E. dispar* was present in the monkey strain. The sequence of the 2.4-kb region in the P19-061405 strain was also determined in a clone cultured axenically and no difference was found compared to before cloning.

### 3.3. Analysis of the serine-rich protein gene

The serine-rich surface protein gene of the P19-061405 strain was amplified and sequenced directly. Repeat patterns of motifs of 3, 4, 8, and 9 amino acids differed from those in reported human isolates [19,22,23]. In the monkey strain, the motif EKASSSDKS is present, compared to EKASSSDNS in human isolates. In the DNKP motif, an AAC codon is used for Asn, whereas in human isolates this codon is AAT. Similarly, the codon for the first serine in the EASSTNKP and EASSTSNS motifs is AGT in the monkey strain and AGC in human isolates.

### 3.4. Analyses of hexokinase genes

Two *HXK* genes of the P19-061405 strain amplified from genomic DNA were cloned and sequenced. The calculated molecular mass and theoretical p*I* were 4.98 kDa and 5.38 in HXK 1, and 4.94 kDa and 4.99 in HXK 2. The deduced amino acid sequences were compared with those of *E. histolytica* and *E. dispar*. Differences between the P19-061405 strain and *E. histolytica* were observed in 3 and 4 of 445 amino acids in HXK 1 and 2, respectively. On the other hand, differences between the monkey strain and *E. dispar* were found for 13 and 15 of the 445 amino acids in HXK 1 and 2, respectively. The p*I* of HXK 1 from the monkey strain differed from that of *E. histolytica* HXK 1, whereas the p*I* of HXK 2 was identical in the two strains.

### 3.5. Analyses of glucose phosphate isomerase genes

Two *GPI* genes from the P19-061405 strain encoded proteins of 546 amino acids with calculated molecular masses of 6.14 kDa. $Lys^{362}$ in the *E. histolytica* GPIs was changed to Glu in the two GPIs of the monkey strain. Two additional differences were found: $Ile^{232}$ and $Val^{330}$ were present in one GPI from the monkey strain, whereas Val and Ala, respectively, were present at these positions in the other GPIs. The theoretical p*I* of the two GPIs from the monkey strain was 6.6, which differed from those of the three *E. histolytica* GPIs.

### 3.6. Analyses of peroxiredoxin genes

Seven different sequences of *PRX* genes were detected in 12 clones from the P19-061405 strain. Using the deduced amino acids, 7 different PRX sequences were identified: 5 had 233 amino acids, 1 had 237 amino acids, and 1 had 229 amino acids. However, none of these sequences were identical to the 6 PRX sequences from the *E. histolytica* HM-1:IMSS strain in the genome database (http://www.tigr.org/tdb/). In the P19-061405 strain, $Val^{156}$ in *E. histolytica* PRXs is replaced with Phe in 5 of the 7 sequences, and $Ala^{161}$ in *E. histolytica* PRXs is replaced with Ser in 6 sequences. In each PRX in the monkey strain, at least one of these two positions was different to *E. histolytica*. In addition, several unique amino acids were found in specific positions in some PRX clones from the P19-061405 strain: $Arg^{130}$, $Ile^{179}$, $Glu^{202}$, $Glu^{217}$, and $Asn^{224}$.

### 3.7. Analyses of isoenzyme patterns

Electrophoretic patterns of four enzymes from the P19-061405 strain are shown in Fig. 4. In HXK, the slower running band in the monkey strain was located between those of *E. histolytica* and *E. dispar*, whereas the mobility of the faster running band was similar to that for HXK from *E. histolytica*. For GPI, only a γ band was observed. Therefore, the band patterns for HXK and GPI appear to be novel in the P19-061405 strain. The mobility of the L-malate:$NADP^+$ oxidoreductase band was same as that for *E. histolytica*/*E. dispar*, and the mobility of the phosphoglucomutase band was the same as that for *E. dispar*.

### 3.8. Virulency of the monkey strain in hamster

When trophozoites of P19-061405 cultured monoxenically with *C. fasciculata* were intrahepatically inoculated into livers of three hamsters, formation of abscesses was observed in all hamsters (Fig. 5). Direct light microscopic examination of the abscess detected moving trophozoites. The presence of many trophozoites was demonstrated in the peripheral region of abscesses in the livers by PAS staining of thin sections (Fig. 6). In two control hamsters, no abscess was detected in livers inoculated with *C. fasciculata* only.

## 4. Discussion

The present study demonstrated that the monkey strain P19-061405 is similar to *E. histolytica*, but the sequences of ribosomal RNA genes were different from those in *E. histolytica* isolated from humans. Differences in 5.8S ribosomal RNA genes and the ITS 1 and 2 regions of *E. histolytica* have been reported among strains HM-1:IMSS, Rahman, and HK-9 [24], but it has

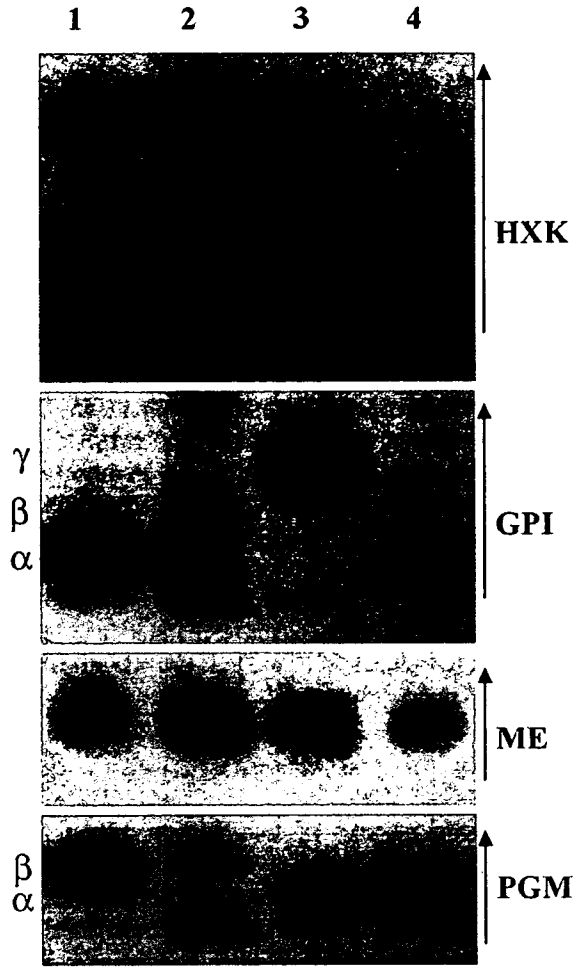


Fig. 4. Isoenzyme patterns of HXK, GPI, L-malate:$NADP^+$ oxidoreductase (ME), and phosphoglucomutase (PGM) from axenically cultured trophozoites of the P19-061405 strain (lane 3). Lane 1, *E. histolytica* HM-1:IMSS strain (Zymodeme II); lane 2, *E. histolytica* SAW1453 strain (Zymodeme XIV); and lane 4, *E. dispar* SAW1734RclAR strain (Zymodeme I). Arrows indicate the direction of migration.

Fig. 6. PAS-stained section of a liver from a hamster that received intrahepatic inoculation of P19-061405 trophozoites. Abscesses are apparent in the bottom half of the photograph, and many PAS-positive trophozoites (arrows) are present in the peripheral region of the abscess. Bar indicates 50 μm.

also been shown that these sequences are identical in 10 strains of *E. histolytica* [25]. In this study, sequence differences in ribosomal RNA genes were not found among human-derived strains of *E. histolytica*, HM-1:IMSS, HK-9, Rahman, and NOT-12. It has also been reported that the sequence of the 18S ribosomal RNA gene is identical in 14 isolates of *E. histolytica* [26]. Therefore, sequences of ribosomal RNA genes seem to be highly conserved in human isolates of *E. histolytica*. The possibility that the sequence difference between P19-061405 and *E. histolytica* is due to PCR or sequencing artifacts, or due to the presence of mixed populations, was ruled out by sequencing and PCR amplification using specific primers, as shown in Fig. 3. The extent of the difference in the 18S ribosomal RNA gene between P19-061405 and *E. histolytica* is only about half that between the genes in *E. histolytica* and *E. dispar*, but this difference appears

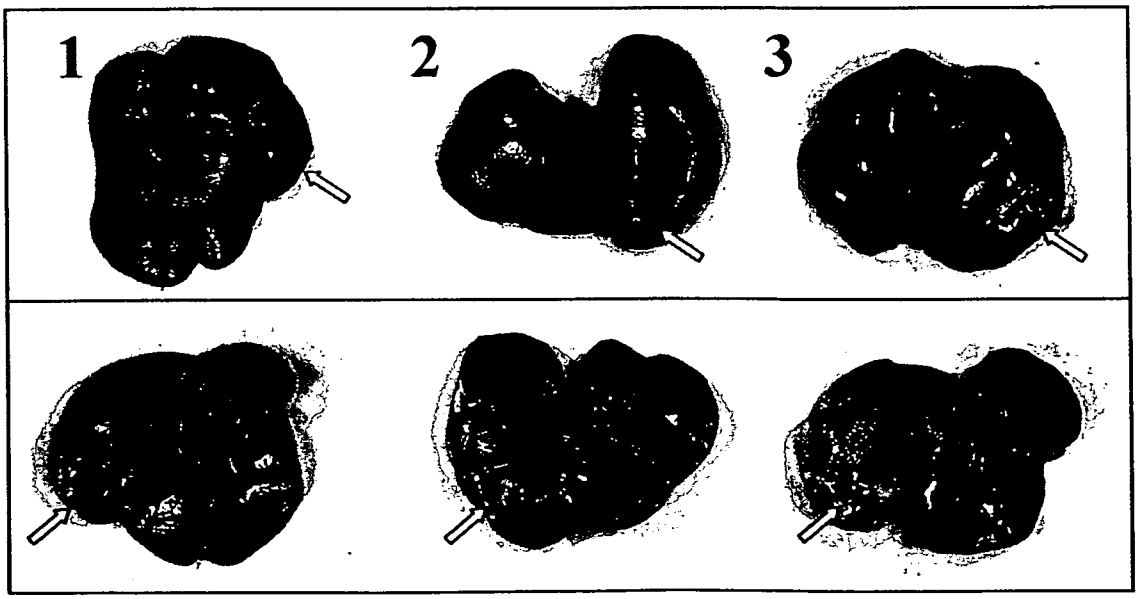


Fig. 5. Livers from 3 hamsters inoculated with trophozoites of the P19-061405 strain 7 days before analysis. Surface (above) and back (below) views are shown. Arrows indicate the location of amebic liver abscesses.